

A Dynamic Market Mechanism for Integration of Renewables and Demand Response

J. Knudsen, J. Hansen, and A.M. Annaswamy

Abstract—The most formidable challenge in assembling a Smart Grid is the integration of a high penetration of renewables. Demand Response, a largely promising concept, is increasingly discussed as a means to cope with the intermittent and uncertain renewables. In this paper, we propose a dynamic market mechanism that reaches the market equilibrium through continuous negotiations between key market players. In addition to incorporating renewables, this market mechanism also incorporates a quantitative taxonomy of demand response devices, based on the inherent magnitude, run-time, and integral constraints of demands. The dynamic market mechanism is evaluated on an IEEE 118 Bus system, a high fidelity simulation model of the Midwestern United States power grid. The results show how the proposed mechanism can be utilized to determine combinations of demand response devices in the presence of intermittent and uncertain renewables with varying levels of penetration so as to result in a desired level of Social Welfare.

Index Terms—Smart Grid, Demand-Side Management, Demand Response, Renewables, Dynamic Market Mechanism

I. INTRODUCTION

THE assembling of Smart Grid, a cyber-enabled transformation proposed for the current grid, faces a number of challenges, the most formidable of which is the integration of a high penetration of Renewable Energy Resources (RERs). The typical operation of a power grid consists of achieving power balance where load is assumed to be fixed, and generation assets are assembled to equal the load, with voltage and frequency control achieved through inertial and terminal voltage stabilization of a large number of synchronous generators. The very first step in this operation, of power balance, is directly affected by the introduction of RERs due to the fact that power generation from RERs is subject to uncertainties and intermittencies.

One of the most promising concepts that is being increasingly discussed is Demand Response (DR), a concept which allows demand to be adjustable [1]-[3], to cope with variations in RERs. A fairly vast literature exists on Demand Response, its potential, and associated challenges and opportunities [4]-[6]. The concept of introducing flexible consumption in market

operations has long been recognized as a highly beneficial one [7], [8]. The idea is then to determine the procedure by which DR can be used concomitantly with RERs so as to ensure an optimal economic dispatch of generation for power balance.

The introduction of intermittency and uncertainty in a smart grid as well as the increasing potential of adjustable demand via DR necessitates a dynamic framework to address the operation, scheduling and financial settlements in the dynamic and uncertain environment. The former brings in issues of strong intermittency and uncertainty, and the latter a feedback structure where demand can be modulated over a range of time-scales. Both of these components are dictating a new look at market mechanisms, with a controls viewpoint enabling a novel framework for analysis and synthesis. This paper proposes a Dynamic Market Mechanism (DMM) together with a portfolio of demand response devices to achieve an optimal economic dispatch in the presence of intermittencies and uncertainties in renewables.

Beginning with a framework that includes price as an underlying state, an attempt is made in this DMM to capture the dynamic interactions between generation, demand, Locational Marginal Price (LMP), and congestion price. The solutions of this dynamic model can be viewed as negotiations between generating companies (GenCos), consumer companies (ConCos), and the Independent System Operator (ISO) that precede convergence to the market equilibrium. The DMM will also include a taxonomy of DR loads, denoted as Buckets, Batteries, and Bakeries (BBB), whose classification is based on distinguishable characteristics of magnitude, run-time, and integral constraints. Conditions under which the DMM is stable and those under which the solutions converge to the market equilibrium are derived. The effect of introducing BBB for various levels of intermittency in RERs is explored. Also investigated is the robustness of the DMM to uncertainties in RERs.

The main idea behind the DMM is that a quantity akin to Real Time Price (RTP) is exchanged between DR-compatible consumers, generators including RERs, and ISO. The use of RTP for incentivizing DR-compatible consumers has been studied extensively (see for example, [9]-[11]). In these papers, the main benefit of RTP is claimed to be a maximum utilization of demand-side assets. As we will show in this paper, the DMM proposed ensures this utilization, with the underlying price quantity arrived at in a different and a stable manner. The benefits of such a DMM over the more standard Optimal Power Flow (OPF) solution, also shown in this paper, lie in the efficient integration of dynamic information about the RERs in terms of both intermittencies and uncertainties, as well as

Manuscript received April 1, 2015.

This work was supported in part by the National Science Foundation grants ECCS-1135815 and EFRI-1441301.

J. Knudsen is with the Section for Automation and Control, Department of Electronic Systems, Aalborg University, Aalborg, Denmark (e-mail: jvk@es.aau.dk)

J. Hansen is a former student in the Department of Electronic Systems, Control and Automation, Aalborg University, Denmark, (e-mail: hansens.jacob@me.com)

A. M. Annaswamy is with the Department of Mechanical Engineering, Active-Adaptive Control Laboratory, Massachusetts Institute of Technology, USA, (e-mail: aanna@mit.edu)

the flexible loads and their various constraints. The DMM presented here builds on earlier work in [12], [1], and [4]. In [12], a DMM was first proposed, but with all flexible demand assumed to be adjustable with no constraints. In [1], shiftable DR loads were addressed as well, and in [4] the scope was extended to include the BBB taxonomy analyzed in this paper. In [12], [1], and [4], validation was limited to either an IEEE 4 Bus or an IEEE 30 Bus. Unlike these earlier papers, we carry out an extensive validation of an extended DMM in this paper using an IEEE 118 Bus system which includes 54 generators, 99 consumers with a varied range of BBB loads, and 186 transmission lines.

Analysis and design of electricity markets have been addressed by a number of researchers ([7], [8], [11], [12], and [13]-[17]). In [13], the authors provide a framework for a dynamic adjustment of the price, but do not take into account the market clearing structure or constraints of capacity, congestion, or power balance. While papers such as [14], [15] focus on the market design in the presence of energy storage, and electric vehicles, dynamic market mechanisms that are affected simultaneously by flexible generation and consumption have not been explored in these works. Market volatility due to real-time prices have been addressed in papers such as [16] and [17]. The focus in these investigations is on the sequence of equilibria arrived at using real-time prices, where the consumers react to the price equilibrium rather than participate actively. Other papers such as [11] have focused on retail markets and the interactions between an energy provider such as a Utility and noncooperative consumers.

The scope of discussions in this paper is at the wholesale level, and is predicated on the assumption that consumer companies exist that are DR-compatible, and can participate in the overall economic dispatch [8], along with renewable generators. A DMM is proposed that prescribes continued negotiations between generators, consumers, and ISO, with active participation of all market entities in the creation of the cleared market price. Conditions under which the market equilibrium can be reached are derived.

While our focus here is on the wholesale market, all of the framework presented can be extended to the retail market under the assumptions of a unique market equilibrium [18] and reliable estimation of demand curves from end-users. Our framework also presupposes that suitable aggregation of various types of demands is feasible (see for example, [19]-[24]), which are for the most part noncooperative [16].

This paper has been organized as follows: In Section II we present a brief introduction to electricity markets. In Section III, the wholesale energy market structure is introduced, which includes modeling of conventional generators, RER generators, BBB consumers, and our proposed Dynamic Market Mechanism. In Section IV numerical studies of an IEEE 118 Bus system are reported to show the effects of the proposed dynamic model. Finally, in Section V and VI we provide discussions and concluding remarks, respectively.

II. INTRODUCTION TO ELECTRICITY MARKETS

An electricity market enables trade of electricity between suppliers and consumers. An efficient market is one where

electricity is traded at a price that minimizes the cost of generation while supplying the entire demand [25]. As electricity cannot be stored in large quantities at the current cost of energy storage, the amount of electricity generated must match the demand at every instant of time to ensure reliability. To ensure adequate amounts of generation also necessitates a forward planning of energy capacity. All of these lead to three broad classes of markets where electricity is traded, which include Energy, Forward Capacity, and Ancillary Services [26].

Energy markets accommodate trade of electricity considering it as an energy commodity. They also ensure just-in-time and just-in-place delivery of electricity to customers. Forward capacity markets are used to provide incentive for building new energy capacity to meet future needs of consumers. Finally, ancillary service markets are used to provide all real-time services needed for reliable delivery of high quality energy. These services include frequency regulation, voltage support and spinning reserve capacity.

In all three classes of electricity markets, electricity suppliers participate by providing their offers based on their costs while consumers, if flexible, participate by providing their demand curves. While the exact procedures used in any given market are region-dependent, trading in all of the above markets can be accomplished using bilateral, auction and/or poolco financial contracts [27]. Bilateral transactions are agreements made between two parties, electricity supplier and electricity consumer, to exchange electricity under mutually agreeable terms for a specified period of time. Trading via auction and poolco contracts usually involves a third party, such as an ISO [28], who oversees the transactions. In both cases the trading agreement is arrived at by the ISO based on best offers, but the distinction between them is that in a poolco market neither ISO nor the participants know what the final price of the trading will be, while in an auction market the price is public during bidding.

A third taxonomy of markets is on the basis of the type of participant in a market, and classified as wholesale and retail markets. Wholesale markets are run by ISO. Power generating companies that sell electricity to load serving entities typically participate in a wholesale market. Participants must bid in quantities of at least 1 MW. The retail electricity market manages the final stage of the power sale from electricity providers to end-use consumers such as small businesses and individual households. Wholesale can be either bilateral, auction or pool, but retail markets are almost completely bilateral in the United States, with regulatory supervision (for example, Department of Public Utilities in the state of Massachusetts [29]).

Regulation market is dedicated to providing frequency regulation in real-time. While energy markets are primarily responsible for balancing demand and generation, any remaining imbalance is taken care of by the regulation market. These markets run once per hour and assign generators responsible for regulation in the next hour. Dispatch of these generators is done through automatic generation control, a fully automated centralized feedback control loop, at the rate of seconds. Forward reserve and real-time reserve markets are used to assign operating reserves throughout the day, which ensure reliable system operation under unpredicted circumstances,

such as equipment failures and faults. We do not address regulation markets or retail markets in this paper.

Our focus in this paper is on wholesale energy markets where decision making occurs at a relatively faster time scale. Energy markets usually consist of decision levels at two different time scales, most important of which are a day-ahead market (DAM) and a real-time market (RTM) [7]. The DAM is settled once every day with hourly schedules for the following day, with a certain market lead time¹. These schedules specify the amounts of electricity to be produced, and consumed, each hour and at what price. Schedules are determined by the ISO to give the lowest price of electricity based on received generation bids, and consumption predictions and bids. Any deviations from the DAM schedules are handled in the RTM. The RTM balances the differences from the DAM schedules when bids and predictions do not match the actual patterns. It runs on a time-scale of minutes (with the market clearing time anywhere between 5 and 15 minutes) and submitted before the start of each operating hour. A common tool used by the ISOs for decision making in the energy market is the Optimal Power Flow, and is described in Section II-A.

As mentioned earlier, a typical energy market procedure consists of participation from electricity suppliers and consumers. The current practice, however, is one where demand is essentially inflexible, whose profile varies with time but otherwise is not adjustable on-demand. An active participation by consumers in electricity markets is an emerging one [31]. As of now, DR is integrated only in DAM (in a few states in the US) at the wholesale level, but not in RTM.

A. Optimal Power Flow

The goal of the Optimal Power Flow method is to determine the schedule of generation over a certain period such that an underlying cost function is optimized [32]. This cost function, denoted as Social Welfare, represents the difference between utility gained by the consumers and the cost incurred by the generators over the period of interest. The optimization of this cost function has to be carried out under both equality and inequality constraints. Equality constraints stem from power balance, as supply must equal demand at all points of the grid and at all times, and inequality constraints from capacity and ramp constraints in the generators and transmission lines. A simplified OPF procedure is described below.

A typical form of Social Welfare, denoted S_W , is given by

$$S_W(x, y) = U(x) - C(y) \quad (1)$$

where x and y denote consumption and generation respectively, $U(\cdot)$ denotes the utility function of consumers, and $C(\cdot)$ denotes the cost function of generators. Equality constraints of the form

$$g_1(x, y, z) = c_1 \quad (2)$$

have to be satisfied, which corresponds to power balance at every node in the grid, where z denotes external variables such

as phase angles, and c_1 is a constant. In addition, inequality constraints of the form

$$\begin{aligned} g_2(x) &\leq c_2 \\ g_3(y) &\leq c_3 \\ g_4(z) &\leq c_4 \end{aligned} \quad (3)$$

have to be simultaneously satisfied as well, where g_i denote capacity and ramp constraints, and c_i are constants for $i = 2, 3, 4$. The OPF problem then corresponds to the maximization of S_W , given by

$$\max_{x \in \mathcal{X}, y \in \mathcal{Y}} S_W(x, y) \quad (4)$$

where \mathcal{X} and \mathcal{Y} denote the set of consumers and generators participating in the energy market. A preceding step to OPF, denoted as the Unit Commitment problem, is typically involved in the determination of the set \mathcal{Y} .

The OPF solution in an energy market then determines the optimal dispatch y^* of generation and x^* optimal consumption, given by the solution $y = y^*$ and $x = x^*$ of (4) subject to the equality constraint in (2) and inequality constraints in (3). The difficulty in the above approach lies in the fact that this optimization is carried out T units ahead of the actual operation time when the generation and consumption occurs. This in turn implies that at this hour, accurate information about $c_i, i = 1, 2, 3, 4$ is assumed to be available. In DAM in ISO-NE, for instance, the OPF solution which consists of the optimal generation schedules for an entire 24 hour period starting at midnight are posted at 6:00 pm of the previous day [33]. That is, information about generation and consumption have to be predicted T hours in advance, where $6 \leq T \leq 29$, accurately. In a real time market, in ISO-NE, $T = 30$ min [33]. Such requirements become difficult to satisfy for several of the generation assets and near impossible for renewables.

In contrast to such an OPF procedure, the DMM that we propose in this paper is an iterative approach, that allows closer to real-time negotiations between generators, consumers, and the ISO, thereby allowing more accurate information that becomes available over the period T to be incorporated. In addition, we include a large class of consumers that are DR-compatible. The role of consumers, x in OPF has been, by and large, represented by utilities participating at the wholesale level. That is, utilities would participate in the optimal power flow by providing the predicted demand x inflexible to the price, i.e. $U(x) = \text{const}$. With emergence of DR programs the set \mathcal{X} is expanding, to include large (typically industrial) customers which would respond to the time of use (TOU) prices or to improve reliability according to the needs of the ISO [34]. With more frequent and uncertain variations in generation, such methods often become inadequate. A systematic and widespread inclusion of demand in market dispatch is becoming increasingly attractive. The nature of demand, however, varies significantly. While many of them are flexible, they are subject to various static and dynamic constraints [4]. Some types of power consumption may be directly adjustable, with overall upper and lower limits in magnitude, but others may have energy constraints, with varying specifications on run-time. To successfully integrate DR-compatible consumers

¹In ISO-NE, as of May 2013, bids are due by 10:00 am and DAM LMPs, schedules, and constraints are published by 13:30 [30]

responding to prices, these varying characteristics (ramping rates, consumption limitations, etc.) have to be considered. Towards this end, the DMM that we propose in this paper assumes that consumers are DR-compatible, and classifies them on the basis of the type of underlying constraints in their consumption. This DMM is an overall iterative approach that allows generators and consumers to respond to suggested prices from the ISO while accommodating all relevant constraints, and can be shown to converge to an efficient market equilibrium. This is discussed in more detail in Section III.

III. A DYNAMIC MARKET MECHANISM

We propose a Dynamic Market Mechanism in this paper for carrying out economic dispatch in a wholesale electricity market. The main participants in this market can be classified into three, (i) consumer company, (ii) generator company, and (iii) ISO. The procedure by which this market mechanism functions is through an iterative set of negotiations, where both ConCos and GenCos submit their suggested bids, which are schedules of consumption and generation, respectively, to which then the ISO responds with suggested prices. The negotiations continue until market equilibrium is reached. All GenCos are assumed to bid their marginal cost i.e., not exercise strategic bidding such as arbitrage. For RER GenCos this further implies that they are competitive [35] and bid to the best of their knowledge i.e., always treating the conditioning forecast as truth.

Section III-A presents models of the consumers, who are assumed to be DR-compatible. Here, we present details of the BBB loads. Section III-B presents generators which include both conventional and RER GenCos. The latter are assumed to have improved forecasts with decreasing prediction horizon. Section III-C addresses the market-clearing procedure, and Section III-D includes details of the market negotiations of the DMM. Stability of the DMM is addressed in Section III-E.

In the remainder of this paper, specifications of quantities used without remark can be found in the nomenclature below.

NOMENCLATURE

N	Total number of nodes.
N_{Dc}	Total number of Bucket ConCos.
N_{Dt}	Total number of Battery ConCos.
N_{Dk}	Total number of Bakery ConCos.
N_{Gc}	Total number of conventional GenCos.
N_{Gr}	Total number of RER GenCos.
T_s	Time step size.
t	Generic time-variable.
t_k	Market-clearing times, $k = 1, 2, \dots$
t_K	Negotiation time-instants, $K = 1, 2, \dots$
T_m	Market-clearing period.
T_d	Negotiation period.
ϕ_n	Set of indices of Bucket ConCos at node n .
φ_n	Set of indices of Battery ConCos at node n .
ψ_n	Set of indices of Bakery ConCos at node n .
θ_n	Set of indices of conventional GenCos at node n .
ϑ_n	Set of indices of RER GenCos at node n .
Ω_n	Set of indices of nodes connected to node n .

A. Consumer Modeling

The consumer companies are modeled based on a flexibility taxonomy denoted *Buckets*, *Batteries* and *Bakeries*, and separates consumers into three classes based on magnitude, run-time, and integral constraints as described below [4].

Buckets: A consumption unit i is defined to be a Bucket if it is a power and energy constrained integrator, a typical example of which are energy storage units such as air conditioner units and refrigeration systems. Each Bucket $i \in D_c = \{1, 2, \dots, N_{Dc}\}$ is assumed to consist of one consuming unit, with its consumption denoted as $P_{Dc_i}(t)$. The associated utility of consumption is assumed quadratic, yielding linearly decreasing marginal utility, as follows:

$$U_{Dc_i}(P_{Dc_i}(t)) = b_{Dc_i}P_{Dc_i}(t) + \frac{c_{Dc_i}}{2}P_{Dc_i}(t)^2 \quad (5)$$

where b_{Dc_i} and c_{Dc_i} are the consumption base and incremental utility, respectively. The power and energy constraints of Bucket i are formally stated in the following definition:

Definition 1 (Bucket): The demand $P_{Dc_i}(t)$ is defined to be of a Bucket if $P_{Dc_i}(t)$ and the stored energy $E_{Dc_i}(t)$ satisfy the following constraints:

$$E_{Dc_i}(t+1) = E_{Dc_i}(t) + T_s P_{Dc_i}(t) \quad (6a)$$

$$\underline{P}_{Dc_i} \leq P_{Dc_i}(t) \leq \overline{P}_{Dc_i} \quad (6b)$$

$$\underline{E}_{Dc_i} \leq E_{Dc_i}(t) \leq \overline{E}_{Dc_i} \quad (6c)$$

where $t = 0, 1, \dots, \infty$, \underline{P}_{Dc_i} , \overline{P}_{Dc_i} , and \underline{E}_{Dc_i} , \overline{E}_{Dc_i} are prespecified lower and upper bounds on the power P_{Dc_i} and energy E_{Dc_i} , respectively. A possible behavior of a Bucket consumer company is illustrated in Fig. 1.

Batteries: A consumption unit i is defined to be a Battery if it is, similar to a Bucket, a power and energy constrained integrator but with an additional constraint of a deadline for achieving a fully charged state. Examples of Batteries are PHEV and swimming pool circulations and filtering systems. Each Battery $i \in D_t = \{1, 2, \dots, N_{Dt}\}$ is assumed to consist of one consuming unit, with its consumption denoted as $P_{Dt_i}(t)$. The associated utility of consumption is assumed quadratic, yielding linearly decreasing marginal utility, as follows:

$$U_{Dt_i}(P_{Dt_i}(t)) = b_{Dt_i}P_{Dt_i}(t) + \frac{c_{Dt_i}}{2}P_{Dt_i}(t)^2 \quad (7)$$

where b_{Dt_i} and c_{Dt_i} are the consumption base and incremental utility, respectively. The power and energy constraints of Battery i are formally stated in the following definition:

Definition 2 (Battery): The demand $P_{Dt_i}(t)$ is defined to be of a Battery if $P_{Dt_i}(t)$ and the stored energy $E_{Dt_i}(t)$ satisfy the following constraints:

$$E_{Dt_i}(t+1) = E_{Dt_i}(t) + T_s P_{Dt_i}(t) \quad (8a)$$

$$0 \leq P_{Dt_i}(t) \leq \overline{P}_{Dt_i} \quad (8b)$$

$$0 \leq E_{Dt_i}(t) \leq \overline{E}_{Dt_i} \quad (8c)$$

$$E_{Dt_i}(T_{i,end}) = \overline{E}_{Dt_i} \quad (8d)$$

where $t = 0, 1, \dots, \infty$, \overline{P}_{Dt_i} , and \overline{E}_{Dt_i} are prespecified upper bounds on the power P_{Dt_i} and energy E_{Dt_i} , respectively, and $T_{i,end} \in \mathbb{N}^+$. A possible behavior of a Battery consumer company is illustrated in Fig. 2.

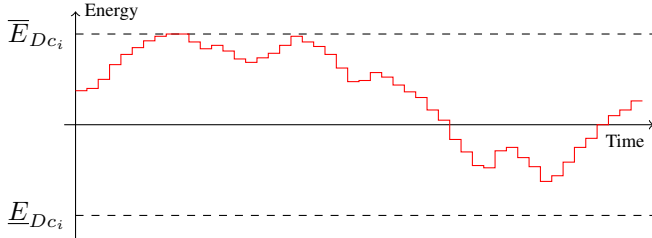


Fig. 1. Illustration of the power and energy properties of a Bucket.

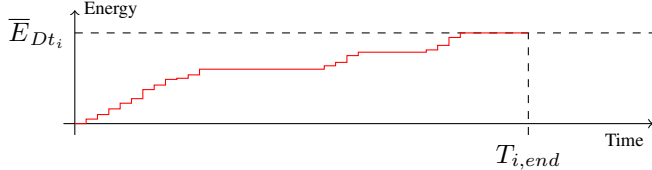


Fig. 2. Illustration of the power and energy properties of a Battery.

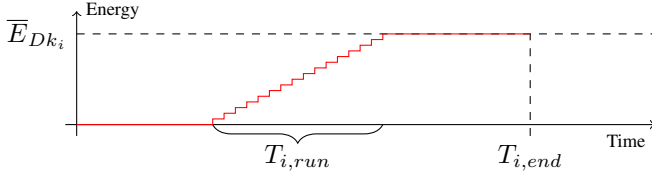


Fig. 3. Illustration of the power and energy properties of a Bakery.

Bakeries: A consumption unit i is defined to be a Bakery if in addition to having constraints on the power, energy, and runtime, the unit is constrained to acquire the energy in a single uninterrupted stretch of constant consumption. Any batch process with a predetermined production cycle such as large industrial production facilities and bakeries, fall under this category. Each Bakery $i \in D_k = \{1, 2, \dots, N_{Dk}\}$ is assumed to consist of one consuming unit, with its consumption denoted as $P_{Dk_i}(t)$. The power and energy constraints of Bakery i are formally stated in the following definition:

Definition 3 (Bakery): The demand $P_{Dk_i}(t)$ is defined to be of a Bakery if $P_{Dk_i}(t)$ and the stored energy $E_{Dk_i}(t)$ satisfy the following constraints:

$$E_{Dk_i}(t+1) = E_{Dk_i}(t) + T_s P_{Dk_i}(t) \quad (9a)$$

$$P_{Dk_i}(t) = \bar{P}_{Dk_i} v_i(t) \quad (9b)$$

$$0 \leq E_{Dk_i}(t) \leq \bar{E}_{Dk_i} \quad (9c)$$

$$E_{Dk_i}(T_{i,end}) = \bar{E}_{Dk_i} \quad (9d)$$

$$0 \leq \sum_{l=t}^{t+T_{i,run}-1} v_i(l) - T_{i,run}(v_i(t) - v_i(t-1)) \quad (9e)$$

where $t = 0, 1, \dots, \infty$, \bar{P}_{Dk_i} and \bar{E}_{Dk_i} are prespecified upper bounds on the power P_{Dk_i} and energy E_{Dk_i} , respectively, $\bar{P}_{Dk_i} \geq 0$, $\bar{E}_{Dk_i} = \bar{P}_{Dk_i} T_{i,run}$, $T_{i,run} \in \mathbb{N}^+$, $T_{i,end} \in \mathbb{N}^+$, $T_{i,end} \geq T_{i,run}$ and $v_i(t) \in \{0, 1\}$ is the binary on/off state of Bakery i . For the purposes of this paper, the sequence $v_i(t)$ is assumed fixed across all Bakeries. A possible behavior of a Bakery consumer company is illustrated in Fig. 3.

B. Generator Modeling

The generator companies are separated into conventional units (e.g., coal and nuclear plants) and RER units (e.g., wind and solar plants) and modeled separately as follows:

Conventional GenCos: For each conventional generator company $i \in G_c = \{1, 2, \dots, N_{Gc}\}$ assumed to consist of one generating unit the generation bid is denoted $P_{Gc_i}(t)$. The associated operation cost as given in (10) is assumed quadratic, yielding linearly increasing marginal cost.

$$C_{Gc_i}(P_{Gc_i}(t)) = b_{Gc_i} P_{Gc_i}(t) + \frac{c_{Gc_i}}{2} P_{Gc_i}(t)^2 \quad (10)$$

where b_{Gc_i} and c_{Gc_i} are the generation base and incremental cost, respectively. The power $P_{Gc_i}(t)$ is subject to two constraints given by

$$\underline{P}_{Gc_i} \leq P_{Gc_i}(t) \leq \bar{P}_{Gc_i} \quad (11a)$$

$$\underline{R}_{Gc_i} \leq P_{Gc_i}(t) - P_{Gc_i}(t-1) \leq \bar{R}_{Gc_i} \quad (11b)$$

where (11a) is a power constraint and (11b) is a rate constraint which when combined, enforce minimum and maximum values of $P_{Gc_i}(t)$ according to the generating units' properties and prior state. Startup and shutdown costs are not included in this model.

RER GenCos: For each renewable energy resource generator company $i \in G_r = \{1, 2, \dots, N_{Gr}\}$ assumed to consist of one generating unit the generation bid is denoted $\hat{P}_{Gr_i}(t)$. The estimated operation cost as given in (12) is assumed quadratic, yielding linearly increasing marginal cost.

$$C_{Gr_i}(\hat{P}_{Gr_i}(t)) = b_{Gr_i} \hat{P}_{Gr_i}(t) + \frac{c_{Gr_i}}{2} \hat{P}_{Gr_i}(t)^2 \quad (12)$$

where b_{Gr_i} and c_{Gr_i} are the generation base and incremental cost, respectively. RER GenCos, in general, have low base cost and negligible incremental costs compared to conventional ones. The bid $\hat{P}_{Gr_i}(t)$ is subject to two constraints given by

$$\underline{P}_{Gr_i} \leq \hat{P}_{Gr_i}(t) \leq \hat{\bar{P}}_{Gr_i}(t) \quad (13a)$$

$$\underline{R}_{Gr_i} \leq \hat{P}_{Gr_i}(t) - P_{Gr_i}(t-1) \leq \bar{R}_{Gr_i} \quad (13b)$$

where (13a) is a power constraint and (13b) is a rate constraint which when combined, enforce minimum and maximum values of $\hat{P}_{Gr_i}(t)$ according to the generating units' properties and prior state. Denoting the true, unknown maximum generation limit as \bar{P}_{Gr_i} , we note that \bar{P}_{Gr_i} may not be known as it is subject to external conditions, e.g., wind speeds in the case of a wind farm. Since \bar{P}_{Gr_i} may not be known during the bidding process, we assume that it is estimated using forecast models as $\hat{\bar{P}}_{Gr_i}(t)$ and satisfies the inequality (13a). That is, assuming that the deviation between this estimate and the true value can be represented as

$$\hat{\bar{P}}_{Gr_i}(t) = (1 + \Delta_{Gr_i}(t)) \bar{P}_{Gr_i} \quad (14)$$

where $\Delta_{Gr_i}(t) \geq -1$, ensure that as the prediction horizon T_H decreases, the estimate $\hat{\bar{P}}_{Gr_i}(T_H)$ approaches its true value \bar{P}_{Gr_i} (see Fig. 4). Recent results show that the accuracy of forecast models improves with decreasing prediction horizon [36], where a Δ_{Gr_i} of 10% can be realized for a prediction horizon of 4 minutes, i.e. $T_H = 4$ min with $\Delta_{Gr_i}(T_H) = 0.1$. The DMM that we propose to use can take advantage of such forecast models by having its negotiations use improved estimates as time proceeds. This is discussed in more detail in Section IV.

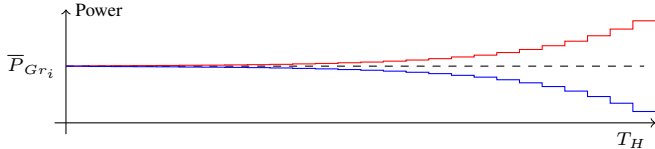


Fig. 4. Example behavior of $\widehat{P}_{Gr_i}(t)$ as $|\Delta_{Gr_i}(t)|$ increases with the prediction horizon T_H . The red line demonstrates $\widehat{P}_{Gr_i}(t)$ with $\Delta_{Gr_i}(t) > 0$ and the blue lines demonstrates $\widehat{P}_{Gr_i}(t)$ with $\Delta_{Gr_i}(t) < 0$.

The inequality $-1 \leq \Delta_{Gr_i}(t) < 0$ represents underestimation i.e., the RER GenCo assumes a maximum generation limit which is smaller than the true limit and the GenCo is assumed to waste a portion of their capacity due to the forecasting error. The inequality $\Delta_{Gr_i}(t) > 0$ represents overestimation i.e., the RER GenCo assumes a maximum generation limit which is higher than the true limit causing lack of power. The GenCo is then penalized for the shortfall by the ISO with the cost of acquiring the missing power from an expensive unit in the reserve market (see for example [37]). The rate constraint is, as seen in (13b), using the actual prior power level and not an estimate since the prior state is known even for a RER generating unit. Startup and shutdown costs are not included in this model and the reserve market is assumed to be always at one's disposal and cleared elsewhere.

C. Market-Clearing

The market-clearing is managed by the ISO, optimizing a cost function subject to system constraints [1]. In addition to the constraints introduced in Sections III-A and III-B, the system constraints include network losses and line capacity limitations. The power flow through lines is constrained by physical parameters and lines are said to be congested when the power flow approaches these constraints. Congestion is directly included in this model, whereas ohmic losses are excluded. The cost function, commonly termed Social Welfare, is designed such that the ISO acts on behalf of ConCos and GenCos, maximizing the utility of ConCos and minimizing the cost of GenCos. As detailed in Section III-B, our model allows power imbalances due to forecasting errors during negotiation, implying that the true cost of generation is found in post-processing. To accommodate this, we denote the intermediate Social Welfare used as cost function in market-clearing by S'_W and the true post-processed Social Welfare by S_W , with the former given by

$$S'_W = \sum_{i \in D_c} U_{Dc_i}(P_{Dc_i}(z(k))) + \sum_{i \in D_t} U_{Dt_i}(P_{Dt_i}(z(k))) - \sum_{i \in G_c} C_{Gc_i}(P_{Gc_i}(z(k))) - \sum_{i \in G_r} C_{Gr_i}(\widehat{P}_{Gr_i}(z(k))) \quad (15)$$

where $z(k)$ denotes the value of a variable z at time $t = t_k$, with $t_{k+1} = t_k + T_m$, and T_m denotes the market-clearing period. The market-clearing optimization problem is then given by

$$\min -S'_W \quad (16)$$

subject to

$$\sum_{i \in \phi_n} P_{Dc_i}(k) + \sum_{i \in \varphi_n} P_{Dt_i}(k) + \sum_{i \in \psi_n} P_{Dk_i}(k) - \sum_{i \in \theta_n} P_{Gc_i}(k) - \sum_{i \in \vartheta_n} \widehat{P}_{Gr_i}(k) + \sum_{m \in \Omega_n} B_{nm}(\delta_n(k) - \delta_m(k)) = 0 \quad \forall n \in N \quad (17a)$$

$$B_{nm}(\delta_n(k) - \delta_m(k)) \leq \overline{P}_{nm} \quad \forall n \in N, \forall m \in \Omega_n \quad (17b)$$

$$\underline{P}_{Dc_i} \leq P_{Dc_i}(k) \leq \overline{P}_{Dc_i} \quad \forall i \in D_c \quad (17c)$$

$$0 \leq P_{Dt_i}(k) \leq \overline{P}_{Dt_i} \quad \forall i \in D_t \quad (17d)$$

$$\underline{P}_{Gc_i} \leq P_{Gc_i}(k) \leq \overline{P}_{Gc_i} \quad \forall i \in G_c \quad (17e)$$

$$\underline{P}_{Gr_i} \leq \widehat{P}_{Gr_i}(k) \leq \overline{P}_{Gr_i}(k) \quad \forall i \in G_r \quad (17f)$$

$$\underline{R}_{Gc_i} \leq P_{Gc_i}(k) - P_{Gc_i}(k-1) \leq \overline{R}_{Gc_i} \quad \forall i \in G_c \quad (17g)$$

$$\underline{R}_{Gr_i} \leq \widehat{P}_{Gr_i}(k) - P_{Gr_i}(k-1) \leq \overline{R}_{Gr_i} \quad \forall i \in G_r \quad (17h)$$

$$\underline{E}_{Dc_i} \leq E_{Dc_i}(k) + T_s P_{Dc_i}(k) \leq \overline{E}_{Dc_i} \quad \forall i \in D_c \quad (17i)$$

$$\underline{E}_{Dt_i}^{\text{ref}}(k+1) \leq E_{Dt_i}(k) + T_s P_{Dt_i}(k) \leq \overline{E}_{Dt_i} \quad \forall i \in D_t \quad (17j)$$

where $\delta_n(k)$ denotes the voltage angle at node n , B_{nm} and \overline{P}_{nm} denotes the susceptance and the maximum capacity of the line from node n to node m , respectively, and $\underline{E}_{Dt_i}^{\text{ref}}(k)$ denotes the minimum reference to guarantee Battery consumer company i satisfy (8d) as specified later. Constraint (17a) enforces nodal power balance, (17b) enforces line capacity limits, (17c)-(17f) enforce power consumption and generation limits for Buckets and Batteries, (17g)-(17h) enforce generation rate limits, and finally (17i)-(17j) enforce consumption energy limits for Buckets and Batteries, respectively. It should be noted that $P_{Gr_i}(k-1)$ in (17h) is the actual value rather than its estimate as these constraints are being evaluated using $k-1$. As the true values of the renewable generation are not known at k , their estimates are used in (17h). $\underline{E}_{Dt_i}^{\text{ref}}(k)$ is a reference value for Battery i and is chosen as follows:

Specification of $\underline{E}_{Dt_i}^{\text{ref}}(k)$: For Battery consumer company i , the fully charged integral constraint (8d) is guaranteed satisfied by a reference for the lower level of stored energy $E_{Dt_i}(k)$ given by

$$\underline{E}_{Dt_i}^{\text{ref}}(k) = \begin{cases} 0 & \text{if } k = 0, \dots, T_{i,start} \\ \overline{P}_{Dt_i}(k - T_{i,start}) & \text{if } k = \begin{cases} T_{i,start} + 1, \\ \dots, T_{i,end} - 1 \end{cases} \\ \overline{E}_{Dt_i} & \text{if } k = T_{i,end}, \dots, \infty \end{cases} \quad (18)$$

where $T_{i,start} = T_{i,end} - \lceil \frac{\overline{E}_{Dt_i}}{\overline{P}_{Dt_i}} \rceil$. This reference guarantees Battery consumer company i to satisfy (8d) while respecting the power limit (8b), and is exemplified in Fig. 5. The choice of $\underline{E}_{Dt_i}^{\text{ref}}(k)$ as in (18) implies that the Battery i has the ability to hold out on consumption until the price is favorable but holding out for too long forces consumption at any cost when k approaches $T_{i,end}$.

We note that, any solution $P_{Dt_i}(k)$ affects the corresponding $E_{Dt_i}(k+1)$ which means constraints on energy has to be fulfilled for $k+1$. Further note that, Bakery consumer companies appear only in (17a) and as fixed values since their consumption is scheduled elsewhere as discussed in Section III-A.

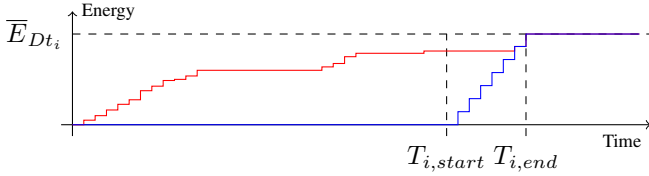


Fig. 5. Illustration of the power and energy properties of a Battery consumer company and its underlying $\underline{E}_{Dt_i}^{\text{ref}}(k)$. The red line shows $E_{Dt_i}(k)$ while the blue line shows $\underline{E}_{Dt_i}^{\text{ref}}(k)$.

D. Market Negotiations of the DMM

We now address the underlying optimization problem which is the optimization of (16) subject to the equality constraint in (17a) and the inequality constraints in (17b)-(17j), at each market-clearing instant k . This is of the form

$$\min f(x) \quad (19a)$$

subject to

$$g_i(x) = 0 \quad i = 1, 2, \dots, n \quad (19b)$$

$$h_j(x) \leq 0 \quad j = 1, 2, \dots, m \quad (19c)$$

where $f(x)$, $g_i(x)$ and $h_j(x)$ are differentiable functions. Formulating the associated Lagrangian as

$$\mathcal{L}(x, \lambda, \mu) = f(x) + \sum_{i=1}^n \lambda_i g_i(x) + \sum_{j=1}^m \mu_j h_j(x) \quad (20)$$

where λ_i and μ_j are the Lagrangian multipliers, Theorem 1 establishes the optimum vector set (x^*, λ^*, μ^*) which can be found by the Karush-Kuhn-Tucker (KKT) conditions [38], [39]. The existence of (x^*, λ^*, μ^*) implies zero duality gap [39], i.e. Slater's condition is satisfied.

Theorem 1 (Saddle-Point Theorem): x^* is a unique solution of (19) if and only if (x^*, λ^*, μ^*) is a saddle-point of $\mathcal{L}(x, \lambda, \mu)$ in $x \geq 0$, $\mu \geq 0$.

The solution (x^*, λ^*, μ^*) can be found using an iterative solution such as the primal-dual interior point method [39] given by

$$x(t+1) = x(t) - \alpha_x \nabla_x \mathcal{L}(x, \lambda, \mu) \quad (21a)$$

$$\lambda(t+1) = \lambda(t) + \alpha_\lambda \nabla_\lambda \mathcal{L}(x, \lambda, \mu) \quad (21b)$$

$$\mu(t+1) = \mu(t) + \alpha_\mu \text{Proj}_\mu(\nabla_\mu \mathcal{L}(x, \lambda, \mu), \bar{\mu}, \underline{\mu}, \epsilon) \quad (21c)$$

where α_x , α_λ and α_μ are positive scalars controlling the amount of change in the gradient direction and $\text{Proj}_\mu(\cdot)$ is a projection operator that ensures non-negativity of μ_j , using bounds $\bar{\mu}$, $\underline{\mu}$, and a boundary-layer thickness ϵ (see (24) for details). The application of this method to the optimization problem corresponding to (16) and (17) forms the DMM.

The starting point for the proposed DMM is the construction of a Lagrangian \mathcal{L} , similar to (20) as

$$\begin{aligned} \mathcal{L} = & C_G(P_G) - U_D(P_D) + \rho_n \left(\sum_{i \in \phi_n} P_{Dc_i} + \sum_{i \in \varphi_n} P_{Dt_i} \right) \\ & + \sum_{i \in \psi_n} P_{Dk_i} - \sum_{i \in \theta_n} P_{Gc_i} - \sum_{i \in \vartheta_n} \hat{P}_{Gr_i} \end{aligned}$$

$$\begin{aligned} & + \sum_{m \in \Omega_n} B_{nm}(\delta_n - \delta_m) \\ & + \gamma_{nm} \left(B_{nm}(\delta_n - \delta_m) - \bar{P}_{nm} \right) \end{aligned} \quad (22)$$

where P_{Gc_i} , \hat{P}_{Gr_i} , P_{Dc_i} , P_{Dt_i} , P_{Dk_i} and δ_n correspond to the states x in (19), ρ_n and γ_{nm} are the Lagrange multipliers and correspond to the Locational Marginal Price (LMP) at node n and the congestion prices of the line from node n to node m respectively, and $C_G(P_G)$ and $U_D(P_D)$ are given by

$$C_G(P_G) = \sum_{i \in G_c} C_{Gc_i}(P_{Gc_i}) + \sum_{i \in G_r} C_{Gr_i}(\hat{P}_{Gr_i}) \quad (23a)$$

$$U_D(P_D) = \sum_{i \in D_c} U_{Dc_i}(P_{Dc_i}) + \sum_{i \in D_t} U_{Dt_i}(P_{Dt_i}) \quad (23b)$$

Finally the projection operator is given by

$$\text{Proj}_y(f(x), \bar{d}_y, \underline{d}_y, \epsilon) =$$

$$\begin{cases} \min \left(\frac{\bar{d}_{y_1}^2 - y_1^2}{\bar{d}_{y_1}^2 - \underline{d}_{y_1}^2}, \dots, \frac{\bar{d}_{y_n}^2 - y_n^2}{\bar{d}_{y_n}^2 - \underline{d}_{y_n}^2} \right) f(x) & \text{if } \begin{cases} f(x) > 0 \wedge \\ \{\bar{d}_{y_1} \leq y_1 \leq \bar{d}_{y_1} \\ \vee \dots \vee \\ \bar{d}_{y_n} \leq y_n \leq \bar{d}_{y_n}\} \end{cases} \\ \min \left(\frac{\underline{d}_{y_1}^2 - y_1^2}{\underline{d}_{y_1}^2 - \bar{d}_{y_1}^2}, \dots, \frac{\underline{d}_{y_n}^2 - y_n^2}{\underline{d}_{y_n}^2 - \bar{d}_{y_n}^2} \right) f(x) & \text{if } \begin{cases} f(x) < 0 \wedge \\ \{\underline{d}_{y_1} \leq y_1 \leq \underline{d}_{y_1} \\ \vee \dots \vee \\ \underline{d}_{y_n} \leq y_n \leq \underline{d}_{y_n}\} \end{cases} \\ f(x) & \text{otherwise} \end{cases} \quad (24)$$

where ϵ is a small positive number, $y = [y_1 \dots y_n]^T$, $\bar{d}_y = [\bar{d}_{y_1} \dots \bar{d}_{y_n}]^T$, $\underline{d}_y = [\underline{d}_{y_1} \dots \underline{d}_{y_n}]^T$, $\bar{d}_y = \bar{d}_y - \epsilon$, and $\underline{d}_y = \underline{d}_y + \epsilon$. The constraints in (17c)-(17j) are accommodated through the use of the projection operator rather than through Lagrange multipliers.

In order to arrive at a solution of (22), which is the overall market equilibrium, we propose an adjustment of the states x in (22), at instances t_K , $K = 0, 1, 2, \dots$, as in (21), as given in (25). It is useful to note that the number of states at each node n is given by the cardinality of ConCo sets ϕ_n , φ_n , and ψ_n , GenCo sets θ_n , and ϑ_n , one for the node voltage angle δ_n , and one for the node LMP ρ_n . The time scale of these adjustments is assumed to be much faster than the market-clearing time, i.e. if we define $t_{K+1} = t_K + T_d$, the negotiation period T_d is assumed to be much smaller than T_m (see Fig. 6). In (25), the conventional generators and renewable generators negotiate individually as P_{Gc_i} and P_{Gr_i} , respectively, and α_x denotes the step sizes corresponding to the variable x .

The goal of the DMM is therefore to start from any t_k and for the state $P_{Gc_i}(t_k)$, $\hat{P}_{Gr_i}(t_k)$, $P_{Dc_i}(t_k)$, $P_{Dt_i}(t_k)$, $P_{Dk_i}(t_k)$, $\delta_n(t_k)$, $\rho_n(t_k)$, and $\gamma_{nm}(t_k)$ to converge to the equilibrium $P_{Gc_i}^*$, $\hat{P}_{Gr_i}^*$, $P_{Dc_i}^*$, $P_{Dt_i}^*$, δ_n^* , ρ_n^* , γ_{nm}^* as the next market-clearing time approaches. That is, we are interested in convergence to the equilibrium as K increases, that is, as $t_k + KT_d$ approaches t_{k+1} .

$$\delta_n(K+1) = \delta_n(K) + \alpha_{\delta_n} \left(- \sum_{m \in \Omega_n} B_{nm} (\rho_n(K) - \rho_m(K) + \gamma_{nm}(K) - \gamma_{mn}(K)) \right) \quad (25a)$$

$$\rho_n(K+1) = \rho_n(K) + \alpha_{\rho_n} \left(\sum_{i \in \phi_n} P_{Dc_i}(K) + \sum_{i \in \varphi_n} P_{Dt_i}(K) + \sum_{i \in \psi_n} P_{Dk_i}(K) - \sum_{i \in \theta_n} P_{Gc_i}(K) + \sum_{i \in \vartheta_n} \widehat{P}_{Gr_i}(K) + \sum_{m \in \Omega_n} B_{nm} (\delta_n(K) - \delta_m(K)) \right) \quad (25b)$$

$$P_{Dc_i}(K+1) = P_{Dc_i}(K) + \text{Proj}_{E_{Dc_i}(K+1)}^{P_{Dc_i}(K+1)} \left(\alpha_{Dc_i} (c_{Dc_i} P_{Dc_i}(K) + b_{Dc_i} - \rho_n(i)), \left[\frac{\overline{P}_{Dc_i}}{\overline{E}_{Dc_i}} \right], \left[\frac{\underline{P}_{Dc_i}}{\underline{E}_{Dc_i}} \right], \epsilon \right) \quad (25c)$$

$$P_{Dt_i}(K+1) = P_{Dt_i}(K) + \text{Proj}_{E_{Dt_i}(K+1)}^{P_{Dt_i}(K+1)} \left(\alpha_{Dt_i} (c_{Dt_i} P_{Dt_i}(K) + b_{Dt_i} - \rho_n(i)), \left[\frac{\overline{P}_{Dt_i}}{\overline{E}_{Dt_i}} \right], \left[\frac{0}{\underline{E}_{Dt_i}^{\text{ref}}(k+1)} \right], \epsilon \right) \quad (25d)$$

$$P_{Gc_i}(K+1) = P_{Gc_i}(K) + \text{Proj}_{R_{Gc_i}(K)}^{P_{Gc_i}(K+1)} \left(\alpha_{Gc_i} (\rho_n(i) - c_{Gc_i} P_{Gc_i}(K) - b_{Gc_i}), \left[\frac{\overline{P}_{Gc_i}}{\overline{R}_{Gc_i}} \right], \left[\frac{\underline{P}_{Gc_i}}{\underline{R}_{Gc_i}} \right], \epsilon \right) \quad (25e)$$

$$\widehat{P}_{Gr_i}(K+1) = \widehat{P}_{Gr_i}(K) + \text{Proj}_{R_{Gr_i}(K)}^{\widehat{P}_{Gr_i}(K+1)} \left(\alpha_{Gr_i} (\rho_n(i) - c_{Gr_i} \widehat{P}_{Gr_i}(K) - b_{Gr_i}), \left[\frac{\widehat{\overline{P}}_{Gr_i}}{\widehat{\overline{R}}_{Gr_i}} \right], \left[\frac{\underline{P}_{Gr_i}}{\underline{R}_{Gr_i}} \right], \epsilon \right) \quad (25f)$$

$$\gamma_{nm}(K+1) = \gamma_{nm}(K) + \text{Proj}_{\gamma_{nm}(K+1)} (\alpha_{\gamma_{nm}} B_{nm} (\delta_n(K) - \delta_m(K)) - \overline{P}_{nm}, \overline{d}_{\gamma_{nm}}, 0, \epsilon) \quad (25g)$$

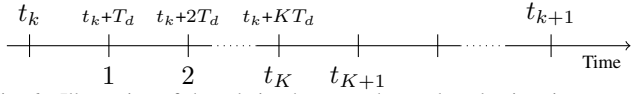


Fig. 6. Illustration of the relation between the market-clearing times t_k and the negotiation time-instants t_K .

Denoting individual elements of a vector z as z_i , the DMM in (25) can be written in state-space form as

$$\begin{bmatrix} x_1(K+1) \\ x_2(K+1) \end{bmatrix} = \begin{bmatrix} A_1 & A_2 \\ 0 & I \end{bmatrix} \begin{bmatrix} x_1(K) \\ x_2(K) \end{bmatrix} + \begin{bmatrix} b_1 \\ b_2(x_1, x_2) \end{bmatrix} \quad (26)$$

where

$$x_1 = [\delta^T \quad \rho^T]^T \quad (27a)$$

$$x_2 = \begin{bmatrix} P_{Dc}^T & P_{Dt}^T & P_{Gc}^T & \widehat{P}_{Gr}^T & \gamma^T \end{bmatrix}^T \quad (27b)$$

$$A_1 = \begin{bmatrix} I & -\alpha_{\delta} A_r^T B_{line} A \\ \alpha_{\rho} A^T B_{line} A_r & I \end{bmatrix} \quad (27c)$$

$$A_2 = \begin{bmatrix} 0 & 0 & 0 & 0 & -\alpha_{\delta} A_r^T B_{line} \\ \alpha_{\rho} A_{Dc} & \alpha_{\rho} A_{Dt} & -\alpha_{\rho} A_{Gc} & -\alpha_{\rho} A_{Gr} & 0 \end{bmatrix} \quad (27d)$$

$$b_1 = [0 \quad P_{Dk}^T A_{Dk}^T \alpha_{\rho}]^T \quad (27e)$$

$$b_2(x_1, x_2) =$$

$$\begin{bmatrix} \text{Proj}_{E_{Dc}(K+1)}^{P_{Dc}(K+1)} \left(\alpha_{Dc} (c_{Dc} P_{Dc}(K) + b_{Dc} - A_{Dc}^T \rho), \left[\frac{\overline{P}_{Dc}}{\overline{E}_{Dc}} \right], \left[\frac{\underline{P}_{Dc}}{\underline{E}_{Dc}} \right], \epsilon \right) \\ \text{Proj}_{E_{Dt}(K+1)}^{P_{Dt}(K+1)} \left(\alpha_{Dt} (c_{Dt} P_{Dt}(K) + b_{Dt} - A_{Dt}^T \rho), \left[\frac{\overline{P}_{Dt}}{\overline{E}_{Dt}} \right], \left[\frac{0}{\underline{E}_{Dt}^{\text{ref}}(k+1)} \right], \epsilon \right) \\ \text{Proj}_{R_{Gc}(K)}^{P_{Gc}(K+1)} \left(\alpha_{Gc} (A_{Gc}^T \rho - c_{Gc} P_{Gc}(K) - b_{Gc}), \left[\frac{\overline{P}_{Gc}}{\overline{R}_{Gc}} \right], \left[\frac{\underline{P}_{Gc}}{\underline{R}_{Gc}} \right], \epsilon \right) \\ \text{Proj}_{R_{Gr}(K)}^{\widehat{P}_{Gr}(K+1)} \left(\alpha_{Gr} (A_{Gr}^T \rho - c_{Gr} \widehat{P}_{Gr}(K) - b_{Gr}), \left[\frac{\widehat{\overline{P}}_{Gr}}{\widehat{\overline{R}}_{Gr}} \right], \left[\frac{\underline{P}_{Gr}}{\underline{R}_{Gr}} \right], \epsilon \right) \\ \text{Proj}_{\gamma(K+1)} (\alpha_{\gamma} (A^T B_{line} A_r \delta - \overline{P}_{nm}), \overline{d}_{\gamma}, 0, \epsilon) \end{bmatrix} \quad (27f)$$

where δ is the $N-1 \times 1$ voltage angle vector, ρ is the $N \times 1$ LMP vector, P_{Dc} is the $N_{Dc} \times 1$ Bucket consumer vector, P_{Dt} is the $N_{Dt} \times 1$ Battery consumer vector, P_{Dk} is the $N_{Dk} \times 1$ Bakery consumer vector, P_{Gc} is the $N_{Gc} \times 1$ conventional generator vector, \widehat{P}_{Gr} is the $N_{Gr} \times 1$ RER generator vector and γ is the $N_t \times 1$ congestion prices vector corresponding to the N_t unique $\delta_n - \delta_m$ equations. Further, A denotes the $N_t \times N$ bus incidence matrix and A_r denotes the $N_t \times N-1$ reduced bus incidence matrix with the column of A corresponding to the reference bus removed. A_{Dc} , A_{Dt} and A_{Dk} denote the $N \times N_{Dc}$, $N \times N_{Dt}$ and $N \times N_{Dk}$, respectively, consumer incidence matrices, where entry $ij = 1$ if the j^{th} consumer is connected to the i^{th} bus and entry $ij = 0$ if the j^{th} consumer is not connected to the i^{th} bus. Similarly, A_{Gc} denotes the $N \times N_{Gc}$ conventional generator incidence matrix and A_{Gr} denotes the $N \times N_{Gr}$ RER generator incidence matrix. B_{line} denotes the $N_t \times N_t$ diagonal line admittance matrix, c 's denote diagonal matrices of incremental coefficients, b 's denote vectors of base coefficients. \overline{P} 's, \overline{E} 's and \overline{R} 's denote vectors of maximum power, energy and rate, respectively. \underline{P} 's, \underline{E} 's and \underline{R} 's denote vectors of minimum power, energy and rate, respectively. \overline{P}_{nm} is the vector of maximum line capacity limits and \overline{d}_{γ} denotes the vector of maximum bounds on γ . Finally, ϵ is a small positive number and α 's are diagonal matrices of appropriate gradient step sizes.

The equilibrium set of the wholesale electricity market given by the game in (25) is defined as

$$E = \{(x_1, x_2) | A_1 x_1 + A_2 x_2 + b_1 = 0 \wedge b_2 = 0\} \quad (29)$$

stating that (x_1^*, x_2^*) is an equilibrium point if and only if $(x_1^*, x_2^*) \in E$. For a sufficiently large K , it follows that if (26) is stable, then the solutions of (27a) and (27b) will be arbitrarily close to the equilibrium.

E. Stability of the DMM

The stability properties of the DMM is addressed in this section. We assume strong duality i.e., zero duality gap, and that the equilibrium $(x_1^*, x_2^*) \in E$ exists.

In the following, we require A_1 in (26) to be Schur stable. It is easy to show that a sufficient condition for Schur stability of A_1 is that at least one of the projected states $P_{Gc_i}, \hat{P}_{Gr_i}, P_{Dc_i}, P_{Dt_i}$ needs to be non projected i.e., must not have reached its projection bounds. By contradiction, we will argue that this is a reasonable requirement as the opposite would pose a system with no flexibility left with either generators or consumers. We assume one of the generators to not hit its projection limits resulting in A'_1 given by

$$A'_1 = \begin{bmatrix} I & -\alpha_\delta A_r^T B_{line} A & 0 \\ \alpha_\rho A^T B_{line} A_r & I & -\alpha_\rho A'_{Gc} \\ 0 & \alpha'_{Gc} A'^T_{Gc} & I - \alpha'_{Gc} c'_{Gc} \end{bmatrix} \quad (30)$$

where A'_{Gc} is the column of A_{Gc} corresponding to the generator which is not projected, c_{Gc} is the incremental cost of that generator and α'_{Gc} is the associated time step of that generator. Using appropriate values for α_δ , α_ρ and α'_{Gc} , A'_1 is Schur stable.

We now introduce a few definitions. Let P be the symmetric solution of $A_1^T P A_1 - P = -I$. Let $\|\alpha_1 A_1^T P \alpha_{Dc} A_{21}\| \leq \beta_1$, $\|\alpha_1 A_1^T P \alpha_{Dt} A_{22}\| \leq \beta_2$, $\|\alpha_1 A_1^T P \alpha_{Gc} A_{23}\| \leq \beta_3$, $\|\alpha_1 A_1^T P \alpha_{Gr} A_{24}\| \leq \beta_4$, $\|\alpha_1 A_1^T P \alpha_\gamma A_{25}\| \leq \beta_5$, $\|\alpha_{Dc} A_{21}^T P \alpha_{Dc} A_{21}\| \leq \beta_6$, $\|\alpha_{Dt} A_{22}^T P \alpha_{Dt} A_{22}\| \leq \beta_7$, $\|\alpha_{Dc} A_{23}^T P \alpha_{Gc} A_{23}\| \leq \beta_8$, $\|\alpha_{Gr} A_{24}^T P \alpha_{Gr} A_{24}\| \leq \beta_9$, $\|\alpha_\gamma A_{25}^T P \alpha_\gamma A_{25}\| \leq \beta_{10}$, $\|\alpha_{Dc} A_{21}^T P \alpha_{Dt} A_{22}\| \leq \beta_{11}$, $\|\alpha_{Dc} A_{21}^T P \alpha_{Gc} A_{23}\| \leq \beta_{12}$, $\|\alpha_{Dc} A_{21}^T P \alpha_{Gr} A_{24}\| \leq \beta_{13}$, $\|\alpha_{Dc} A_{21}^T P \alpha_\gamma A_{25}\| \leq \beta_{14}$, $\|\alpha_{Dt} A_{22}^T P \alpha_{Gc} A_{23}\| \leq \beta_{15}$, $\|\alpha_{Dt} A_{22}^T P \alpha_{Gr} A_{24}\| \leq \beta_{16}$, $\|\alpha_{Dt} A_{22}^T P \alpha_\gamma A_{25}\| \leq \beta_{17}$, $\|\alpha_{Gc} A_{23}^T P \alpha_{Gr} A_{24}\| \leq \beta_{18}$, $\|\alpha_{Gc} A_{23}^T P \alpha_\gamma A_{25}\| \leq \beta_{19}$, and $\|\alpha_{Gr} A_{24}^T P \alpha_\gamma A_{25}\| \leq \beta_{20}$ where α_1 is a diagonal matrix containing α_δ , α_ρ , and α'_{Gc} and the columns of A_2 are denoted $A_{21}, A_{22}, A_{23}, A_{24}$, and A_{25} , respectively. Furthermore, let $y_1 = x_1 - x_1^*$, $y_{21} = P_{Dc} - P_{Dc}^*$, $y_{22} = P_{Dt} - P_{Dt}^*$, $y_{23} = P_{Gc} - P_{Gc}^*$, $y_{24} = \hat{P}_{Gr} - \hat{P}_{Gr}^*$, $y_{25} = \gamma - \gamma^*$, $y_2 = [y_{21}^T \ y_{22}^T \ y_{23}^T \ y_{24}^T \ y_{25}^T]^T$, and define

$$\Omega_{\max} \equiv \{(y_1, y_2) \mid \|y_{21}\| \leq \bar{d}_{Dc}, \|y_{22}\| \leq \bar{d}_{Dt}, \|y_{23}\| \leq \bar{d}_{Gc}, \|y_{24}\| \leq \bar{d}_{Gr}, \|y_{25}\| \leq \bar{d}_\gamma\} \quad (31)$$

$$\Omega_{\min} \equiv \{(y_1, y_2) \mid V(y_1(k)) \leq \lambda_{\min}(P)\eta^2, \|y_{21}\| \leq \bar{d}_{Dc}, \|y_{22}\| \leq \bar{d}_{Dt}, \|y_{23}\| \leq \bar{d}_{Gc}, \|y_{24}\| \leq \bar{d}_{Gr}, \|y_{25}\| \leq \bar{d}_\gamma\} \quad (32)$$

$$\eta = \frac{\eta_1}{2} + \frac{1}{2} \sqrt{\eta_1^2 + 4\eta_2} \quad (33)$$

$$\eta_1 = 2\bar{d}_{Dc}\beta_1 + 2\bar{d}_{Dt}\beta_2 + 2\bar{d}_{Gc}\beta_3 + 2\bar{d}_{Gr}\beta_4 + 2\bar{d}_\gamma\beta_5 \quad (34)$$

$$\begin{aligned} \eta_2 = & 2\bar{d}_{Dc}^2\beta_6 + 2\bar{d}_{Dt}^2\beta_7 + 2\bar{d}_{Gc}^2\beta_8 + 2\bar{d}_{Gr}^2\beta_9 + 2\bar{d}_\gamma^2\beta_{10} \\ & + 2\bar{d}_{Dc}\beta_{11}\bar{d}_{Dt} + 2\bar{d}_{Dc}\beta_{12}\bar{d}_{Gc} + 2\bar{d}_{Dc}\beta_{13}\bar{d}_{Gr} \\ & + 2\bar{d}_{Dc}\beta_{14}\bar{d}_\gamma + 2\bar{d}_{Dt}\beta_{15}\bar{d}_{Gc} + 2\bar{d}_{Dt}\beta_{16}\bar{d}_{Gr} \\ & + 2\bar{d}_{Dt}\beta_{17}\bar{d}_\gamma + 2\bar{d}_{Gc}\beta_{18}\bar{d}_{Gr} + 2\bar{d}_{Gc}\beta_{19}\bar{d}_\gamma \\ & + 2\bar{d}_{Gr}\beta_{20}\bar{d}_\gamma \end{aligned} \quad (35)$$

Theorem 2: Let strong duality hold. Then the equilibrium $(x_1^*, x_2^*) \in E$ of the DMM in (26) is stable for all initial

conditions in Ω_{\max} if A'_1 is Schur stable. In addition all trajectories will converge to Ω_{\min} .

Proof: The following Lemma is useful:

Lemma 1: If $\dot{y} = \text{Proj}_y(f(x), \bar{d}_y, \underline{d}_y, \epsilon)$ then $\underline{d}_{y_1} \leq \|y_1(t_0)\| \leq \bar{d}_{y_1}, \dots, \underline{d}_{y_n} \leq \|y_n(t_0)\| \leq \bar{d}_{y_n}$ implies $\underline{d}_{y_1} \leq \|y_1(t)\| \leq \bar{d}_{y_1}, \dots, \underline{d}_{y_n} \leq \|y_n(t)\| \leq \bar{d}_{y_n}$ for all $t \geq t_0$.

Proof: Let $V(y) = \frac{1}{2}y^2$ such that $\dot{V}(y) = yf(x)$. It is easily seen that (24) ensures that \dot{V} will gradually approach zero when y approaches \underline{d}_y or \bar{d}_y . ■

The rate change of the positive definite Lyapunov function $V(y(k)) = y_1^T(k)P y_1(k)$ is given by

$$\Delta V(y(k)) = y_1^T(k+1)P y_1(k+1) - y_1^T(k)P y_1(k) \quad (36)$$

From this point on we will suppress the explicit time dependence of time varying parameters and we get

$$\begin{aligned} \Delta V(y_1) = & (A'_1 y_1 + A_{21} y_{21} + A_{22} y_{22} + A_{23} y_{23} + A_{24} y_{24} \\ & + A_{25} y_{25})^T P (A'_1 y_1 + A_{21} y_{21} + A_{22} y_{22} \\ & + A_{23} y_{23} + A_{24} y_{24} + A_{25} y_{25}) - y_1^T P y_1 \end{aligned} \quad (37)$$

Since A'_1 is Schur stable the right-hand side of (37) can be rewritten using the definitions of β_1 through β_{20} along with the projection bounds on y_2 as follows

$$\begin{aligned} \Delta V(y_1) = & -\|y_1\|^2 + 2\|y_1\|(\bar{d}_{Dc}\beta_1 + \bar{d}_{Dt}\beta_2 + \bar{d}_{Gc}\beta_3 \\ & + \bar{d}_{Gr}\beta_4 + \bar{d}_\gamma\beta_5) + 2(\bar{d}_{Dc}^2\beta_6 + \bar{d}_{Dt}^2\beta_7 + \bar{d}_{Gc}^2\beta_8 \\ & + \bar{d}_{Gr}^2\beta_9 + \bar{d}_\gamma^2\beta_{10} + \bar{d}_{Dc}\beta_{11}\bar{d}_{Dt} + \bar{d}_{Dc}\beta_{12}\bar{d}_{Gc} \\ & + \bar{d}_{Dc}\beta_{13}\bar{d}_{Gr} + \bar{d}_{Dc}\beta_{14}\bar{d}_\gamma + \bar{d}_{Dt}\beta_{15}\bar{d}_{Gc} \\ & + \bar{d}_{Dt}\beta_{16}\bar{d}_{Gr} + \bar{d}_{Dt}\beta_{17}\bar{d}_\gamma + \bar{d}_{Gc}\beta_{18}\bar{d}_{Gr} \\ & + \bar{d}_{Gc}\beta_{19}\bar{d}_\gamma + \bar{d}_{Gr}\beta_{20}\bar{d}_\gamma) \end{aligned} \quad (38)$$

Using definitions for η_1 and η_2 we obtain

$$\Delta V(y_1) = -\|y_1^2\| + \|y_1\|\eta_1 + \eta_2 \quad (39)$$

From (39) follows boundedness of y_1 and convergence of all trajectories to Ω_{\min} . Furthermore, it is apparent that Ω_{\min} is a subset of Ω_{\max} , since y_1 is arbitrary in Ω_{\max} and specified by η in Ω_{\min} . ■

IV. CASE STUDIES

We now illustrate the features of the DMM using a case study. We will show that our DMM is capable of identifying the combination of DR units that will be needed, as the RERs vary. Variations in the overall penetration level will be considered, as well as in the intermittency of a given RER. Also considered are uncertainties in the RER. It will be shown that in all cases, the DMM will identify the combination of BBB that is necessary to achieve optimal economic dispatch.

The case studies reported below use a modified IEEE 118 Bus system², a high fidelity simulation of the Midwestern US Power Grid as of December 1962. The modified bus system consists of 54 generators, 99 consumers, and 186 transmission lines connected as shown in Fig. 7. The modified IEEE 118 Bus diagram uses the following syntax: Each generator is

²Unmodified bus data: <http://ee.washington.edu/research/pstca/>

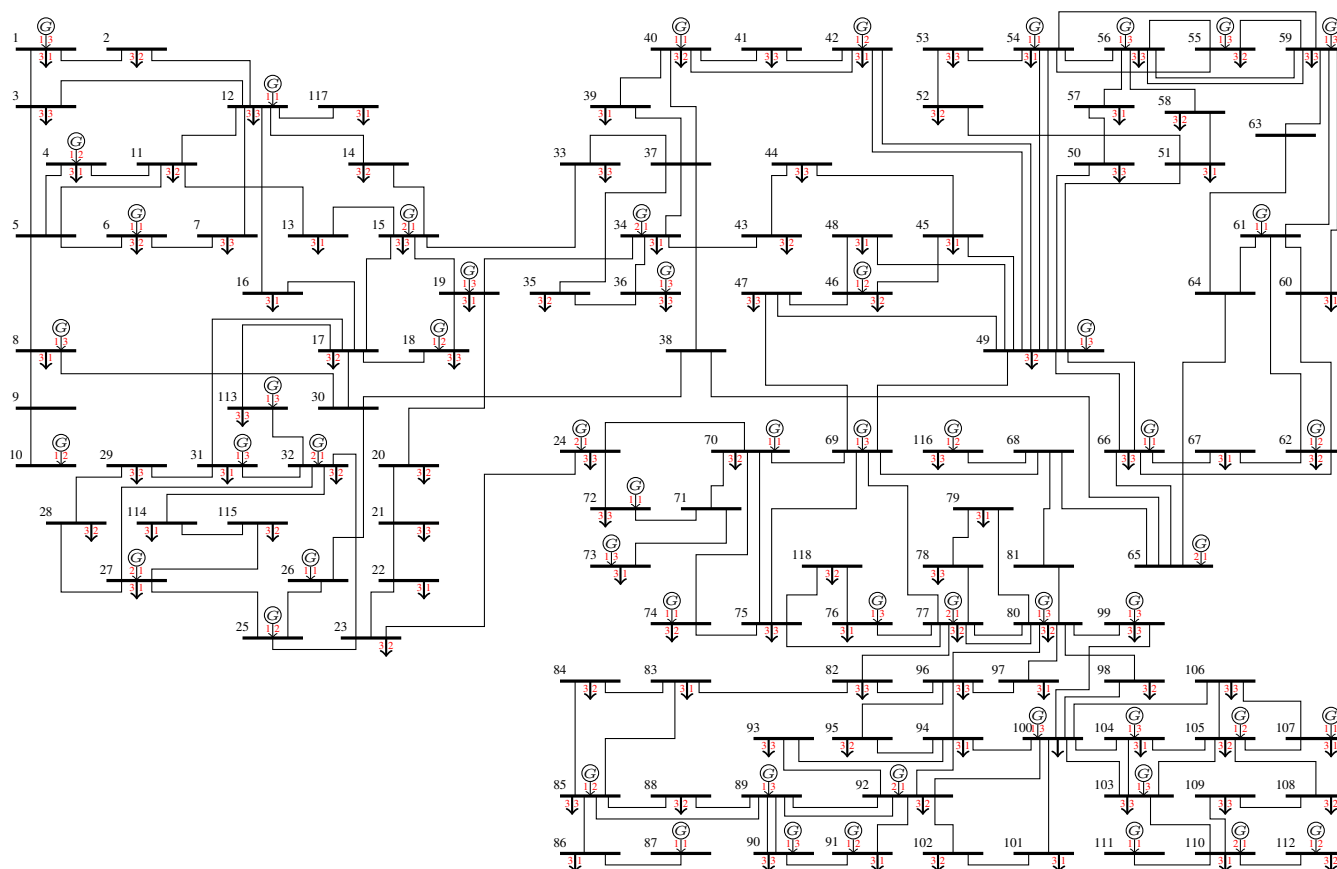


Fig. 7. Modified IEEE 118 Bus diagram

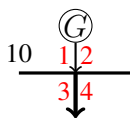


Fig. 8. Example of the syntax of the modified IEEE 118 Bus diagram. 10 is the bus number, 1 is the class of generator, 2 is type of generator, 3 is the class of consumer, and 4 is the type of consumer.

associated with two numbers in red. The left one indicates the class of generator, either conventional or RER. The right number indicates the type of that generator. Each consumer is also associated with two numbers in red. The left one indicates the class of consumer, either a Bucket, a Battery, or a Bakery. The right number indicates the type of the consumption unit, based on its power and energy rating. Conventional and RER generators are numbered 1 and 2, respectively, while Buckets, Batteries, and Bakeries are numbered 1, 2, and 3, respectively. An example is given in Fig. 8. Definitions of the types for both generators and consumers can be found in Appendix A. The modified IEEE 118 Bus system shown in Fig. 7, is made up of 45 conventional generators (13 of Type 1, 12 of Type 2, and 20 of Type 3), 9 RER generators (all of Type 1), 0 Bucket consumers, 0 Battery consumers, and 99 Bakery consumers (33 of Type 1, 33 of Type 2, and 33 of Type 3). Any alterations from this setup will be specified in the corresponding cases.

The three categories of BBB consumption units are introduced into the 118 Bus system in the following manner.

The locations of Bakeries, 99 in number, are assumed to be fixed, and as indicated in the IEEE 118 Bus system shown in Fig. 7. This is denoted as a B distribution. These 99 Bakeries were chosen to be one of three types defined in Table XI in Appendix A with the type distribution chosen in a uniform manner. To this distribution, 30 Batteries are introduced at locations as shown in Table I. This is denoted as a BB distribution. Finally, 10 Buckets as defined in Table II is introduced at various locations. The choices of the locations of the Bakeries (in Fig. 7), Batteries in Table I and Buckets in Table II were fairly arbitrary. The choices of the distribution of the 30 Batteries across the three types, described in Table X in Appendix A, were uniform.

When introducing Battery consumption, we replace the equivalent amount of Bakery consumption from the system by removing the Bakery at a node where we add a Battery. This is done to keep the overall consumption at the same level. However, while introducing Bucket consumption, we simply add Bucket consumers as their flexibility, as given in Definition 1, does not compare to the consumption of Bakery or Battery consumers. It should be noted that the number of Buckets, Batteries, and Bakeries was chosen arbitrarily. A second level of optimization of these numbers may be feasible, but is not addressed in this paper.

The different cases considered in this paper are grouped so as to illustrate the behavior of the proposed DMM in the presence of (A) uncertainties in RERs, and (B) intermittencies

TABLE I
ADDITIONS OF BATTERY CONSUMERS TO THE MODIFIED 118 BUS SYSTEM FOR S CASES.

Bus	Type
1, 13, 22, 34, 45, 54, 67, 79, 91, 100	1
17, 28, 40, 49, 58, 74, 84, 95, 104, 114	2
21, 33, 44, 53, 66, 78, 90, 99, 108, 118	3

TABLE II
ADDITIONS OF BUCKET CONSUMERS TO THE MODIFIED 118 BUS SYSTEM FOR S CASES.

Bus	Type
6, 20, 33, 47, 59, 76, 86, 97, 105, 116	1

in RERs. All cases are assumed to correspond to the wholesale Real-Time Market, with a market-clearing time of 5 minutes and evaluated over a 1-hour period.

First, the impact of uncertainty in RER generation availability is studied by varying the forecasting errors included in the model by Δ_{Gr_i} in (14). Second, the impact of intermitencies in RER generation availability is studied over a range of RER penetration levels, and over a range of intermitency of the RER generators. The intermitency in RER is implemented as shown in Fig. 9, where over a 5 minute period in the entire hour, it is assumed that the maximum power available can take any one of three different values. This reflects variations due to extreme weather conditions [40]. The baseline corresponds to the solid red line where there is no intermitencies. The dashed red line pose a drop in RER generation availability of 30%, the dashed blue line pose a drop of 60% and the dashed orange line a drop of 90%. In each case, it is assumed that DR consumers from BBB introduced in III-A are available.

Three levels of RER penetration, of 15%, 30%, and 45% are introduced. When increasing the RER penetration level, we replace the capacity of conventional generators with RER generators but keep the overall generation capacity equal across all configurations. Each of these penetration levels is assumed to be realized in the 118 Bus system in the following manner. A 15% penetration level is realized by choosing the generators, both conventional and RER, as shown in Figure 7. 30% and 45% RER penetration levels are realized by modifying the generators as described in Table III, and Table IV, respectively. For each of these penetration levels, we introduce three levels of intermitencies. The intermitency profiles are, as described earlier, shown in Fig. 9.

The DMM proposed in (26) and (27) is now applied to the modified IEEE 118 Bus. Initial values for all α constants are set at 0.001 and all state variables are set at arbitrary values within the bound of the specific variable. If the variable is unbounded the initial condition is set at zero. It was observed that in all cases, the DMM converged to the market equilibrium if it exists. Cases where the equilibrium did not exist are denoted as being "infeasible". Before proceeding with the analysis of the DMM in the presence of uncertainties and intermitencies in the RER, we first present the results at one

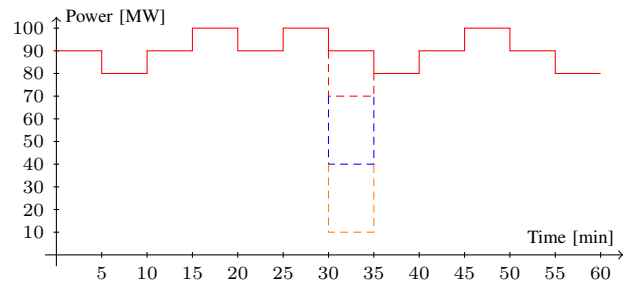


Fig. 9. Behavior of $\bar{P}_{Gr}(k)$ used for case studies. The solid red line is the basis, the dashed red line pose a drop of 30%, the dashed blue line pose a drop of 60% and the dashed orange line pose a drop of 90%.

TABLE III
ADDITIONS OF RER GENERATORS (CLASS 2) AND REMOVALS OF CONVENTIONAL GENERATORS (CLASS 1) FROM THE MODIFIED 118 BUS SYSTEM FOR S CASES WITH 30% RER PENETRATION LEVEL.

Bus	Class	Type
6, 8, 26, 42, 59, 69, 85, 96, 105	2	1
6, 26	1	1
42, 85, 105	1	2
8, 59, 69	1	3

TABLE IV
ADDITIONS OF RER GENERATORS (CLASS 2) AND REMOVALS OF CONVENTIONAL GENERATORS (CLASS 1) FROM THE MODIFIED 118 BUS SYSTEM WITH 30% RER PENETRATION LEVEL FOR S CASES WITH 45% RER PENETRATION LEVEL.

Bus	Class	Type
1, 18, 23, 46, 54, 62, 73, 74, 100	2	1
54, 74	1	1
18, 46, 62	1	2
1, 73, 100	1	3

operating condition below.

The steady-state values of P_{Gc_i} , \hat{P}_{Gr_i} , P_{Dk_i} , P_{Dt_i} , E_{Dt_i} , P_{Dc_i} , and E_{Dc_i} are shown in Figs. 10 and 11. In both figures, the results correspond to a total of 60 minutes, with 12 market clearings in total, one occurring every 5 minutes. The generation mix, Bakery power, Battery power, Battery energy, Bucket power, and Bucket energy needed to achieve market clearing at each of the 12 instants are shown in Tables VI-VIII. The same information is provided as a snap-shot in a 3-dimensional format in Fig. 11 including the accumulated power levels of all the 11 assets in the system throughout all the 12 market-clearing instances. The 11 assets include RER generation type 1, conventional generation type 1, conventional generation type 2, conventional generation type 3, Bakery consumption type 1, Bakery consumption type 2, Bakery consumption type 3, Battery consumption type 1, Battery consumption type 2, Battery consumption type 3, and Bucket consumption type 1. All results shown in Figs. 10 and 11 correspond to a 15% RER penetration level, a 90% RER drop between the 30 minute and the 35 minute window, and a BBB configuration.

In Fig. 10(a), we see the output of each of the 54 generators for each market-clearing. The generators are colored according

to class and type; green is RER generation, red is conventional generation type 1, magenta is conventional generation type 2, and blue is conventional generation type 3 (see Appendix A for a definition of type). Shades within each color distinguish individual generators.

In Fig. 10(b), we see the Bakery consumption of each of the 69 Bakery consumers included in the 118 Bus system. The consumption is once again colored according to type; red is Bakery consumption type 1, green is Bakery consumption type 2, and blue is Bakery consumption type 3 (see Appendix A for a definition of types). Shades within each color distinguish individual consumption units. Similarly in Figs. 10(c) and 10(d), we see power consumption of each of the 30 Battery consumers and energy consumption of these consumers, respectively. The color red is Battery consumption type 1, green is Battery consumption type 2, and blue is Battery consumption type 3.

In Figs. 10(e) and 10(f), the Bucket power and energy consumptions of each of the 10 Buckets are shown, respectively, which are all of the same type.

Figs. 10 and 11 show how the flexible consumption with the BBB configuration follows the low-cost RER generation when available. In particular, at the 7th market clearing instance (at the 30th minute), where the RER generation availability drops as given by the dashed orange curve on Fig. 9, Figs. 10 and 11 show how the flexible consumers aid in balancing the system. The Battery consumers turn off, while the Bucket consumers act as generators to maintain power balance with limited ramping of conventional generators. As higher RER generation becomes available in the subsequent market-clearings, the Battery consumers turn back on to ensure reaching the individual maximum energy level within the deadline.

A. Uncertainty Impacts

As mentioned in Section III-B, RER Generation negotiations include an uncertainty Δ_{Gr_i} as in (14). It was argued in Section III-B that this uncertainty reduces to zero with the prediction horizon T_H , as demonstrated in Fig. 4. In other words, between any two market-clearing instants t_k and t_{k+1} , as negotiations proceed, the magnitude of $\Delta_{Gr_i}(t)$ reduces. In contrast, in an OPF, the estimate $\hat{P}_{Gr_i}(t)$ is set to

$$\hat{P}_{Gr_i}(t) = (1 + \Delta_{Gr_i}(k)) \bar{P}_{Gr_i} \quad \forall t \in [k, k+1] \quad (40)$$

with the value of $\Delta_{Gr_i}(k)$ set at a constant value corresponding to the forecast error prevalent at t_k over the whole interval $[k, k+1]$. In Case studies *U1* and *U2*, we compare the DMM and OPF for different types of uncertainties. The IEEE 118 Bus system as in Fig. 7 is used with the maximum power limit of the RER generators following the solid red line in Fig. 9.

Case Study U1: We compared the performances of the DMM and OPF for the case when the forecast error was 5% when the negotiations began, and reduced to 1% 1 minute prior to the market-clearing time. That is, $\Delta_{Gr_i}(t_k) = 0.05$, $\Delta_{Gr_i}(t_{k+1} - T_H^*) = 0.01$ where $T_H^* = 1$ min. The positive forecasting error represents overestimation, leading to a lack of power which is assumed to be acquired in the reserve market.

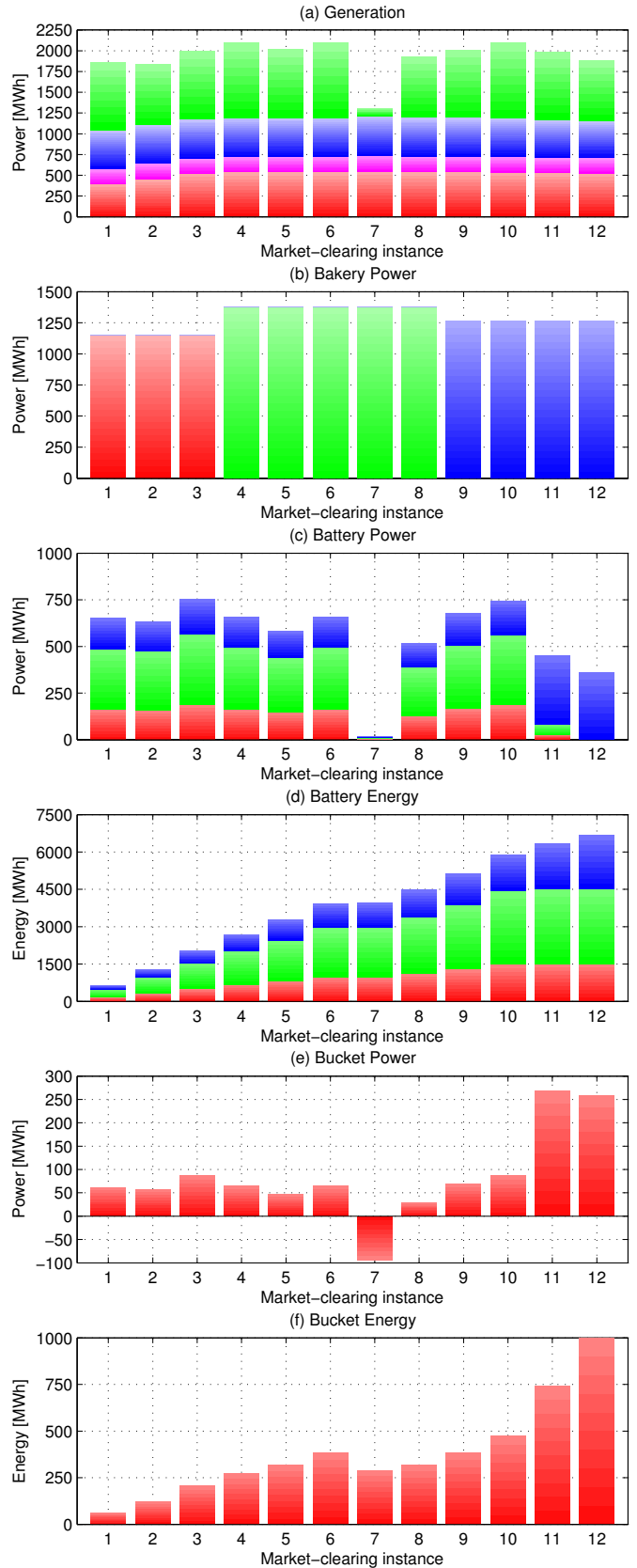


Fig. 10. Market-clearing results during one hour with a 5 minute market-clearing time in a system with 15% RER penetration level, BBB flexibility configuration and 90% RER generation availability drop. Colors distinguish class and type of generators/consumers, shades distinguish individual generators/consumers.

TABLE V
RESULTS OF CASE STUDIES U1 AND CASE U2.

Case	Social Welfare Change
U1	17.1%
U2	9.5%

Based on historical reserve cost from PJM³ the cost of the reserve market is set at 10 times the cost of the most expensive generator. The comparison of the DMM and OPF is carried out using Social Welfare. The results obtained are shown in Table V, which illustrates that DMM results in a 17.1% increase compared to the OPF.

Case Study U2: Similar to Case Study U1, another comparison of the DMM and OPF is for the case when $\Delta_{Gr_i}(K) = -5\%$ when the negotiations begin and decreases to -1% over a 4 minute period, i.e. $T_H = 4$ minutes. The negative forecasting error represents underestimation, leading to a waste of RER generation capacity and unnecessary high amount of power being generated from conventional generators. The results obtained are shown in Table V, which illustrates that DMM results in a 9.5% increase compared to the OPF. The change in Case Study U1 is greater than in Case Study U1 as acquiring power in the reserve market impose a larger additional cost than a dispatch with more power coming from conventional generators.

B. Intermittency Impacts

In this section, we explore the performance of the DMM in the presence of intermittencies in the RER.

Case Study I1: Here, we assume that there is a 30% drop in the available RER from minute 30 to minute 35, over a 1 hour period of study (corresponding to the red dashed line in Fig 9). We evaluate the behavior of the DMM with RER penetration levels at 15%, 30% and 45%. The resulting performance of the DMM is summarized in Table VI. The entries in the table correspond to the improvement in S_W compared to that in a nominal case, which corresponds to S_W obtained at a 15% RER penetration level, with the only consumption units corresponding to Bakeries, and a 30% drop in RER level i.e., the (1,3) entry in Table VI. Table VI shows the three kinds of BBB distribution that is needed in order to accommodate the varying levels of RER penetration (B denotes the use of Bakeries only, BB denotes Bakeries and Batteries, and BBB denotes the use of all three consumption units Bakeries, Batteries, and Buckets). Each of the nine entries was a result of the DMM solution. Entry (1,2) did not result in a feasible solution.

Case Study I2: Here, we assume that there is a 60% drop in the available RER over the same period as in Case Study I1 (corresponding to the blue dashed line in Fig. 9). We once again evaluate the behavior of the DMM at the three RER penetration levels as in Case Study I1. The resulting performance of the DMM is summarized in Table VII. The same nominal case as in Case Study I1 was used in order to

compute the entries of Table VII. The higher magnitude of the drop can be seen to result in making the use of Bakeries alone entirely infeasible i.e., all entries in the first column in Table VII did not result in a feasible solution. It should be noted that the increase in the Social Welfare with the introduction of Batteries and Buckets are somewhat inflated, as the utility costs of Bakeries are not included in the definition of S_W .

Case Study I3: Here, we assume that there is a 90% drop in the available RER over the same period as in Case Study I1 (corresponding to the orange dashed line in Fig. 9), and evaluate the DMM for the same RER penetration levels as in Case studies I1 and I2. The resulting performance of the DMM is summarized in Table VIII. More combinations can be observed to be infeasible, compared to Tables VI and VIII, which is to be expected.

Observations

The following are some important observations to be made from Tables VI-VIII.

- Tables VI-VIII show that S_W increases as the RER drop
- Across Tables VI-VIII, we see smaller improvements in Social Welfare when the drop in RER generation availability increases. This is logical as increased drops implies less low-cost RER generation in the system.
- Tables VI-VII show that the BB configuration results in increased improvements in S_W even as the RER penetration level raises. This is primarily due to the injection of more low-cost RER generation capacity in the system i.e., reduced reliance on higher-cost conventional generator.
- A row-wise comparison of Tables VI-VII for BB and BBB configurations show improvements across the board with the addition of Buckets. The exact relative improvements depend highly on the constraint in each scenario.
- Across Tables VI-VIII, we see more scenarios becoming infeasible as the drop in RER generation availability increases. In the case of 90% drop, for instance, only 15% RER penetration is feasible if no Buckets are available.
- Table VI shows that if only Bakeries were to be used, a 30% RER penetration level becomes infeasible. This underscores two obvious points, which is that relying on RER generation is possible if the corresponding drop is not too large for them to still cover any inflexible consumption and that the model can capture properties of the grid, such as inflexibility due to ramping limits.

V. COMPARISON WITH ALTERNATE APPROACHES

We now provide a brief discussion on the proposed model in comparison with an alternative proposal.

The DMM approach implements, and relies on, LMP that is arrived at by taking full advantage of the flexibility provided on the demand-side. The argument behind the use of the LMP is that it leads to nodal power balance, i.e. it denotes the price that makes generation and consumption match. Instead of using LMP, one could have used any price driven incentive signal, and this signal need not be the true price but merely be

³<http://www.pjm.com/markets-and-operations/data-dictionary.aspx>

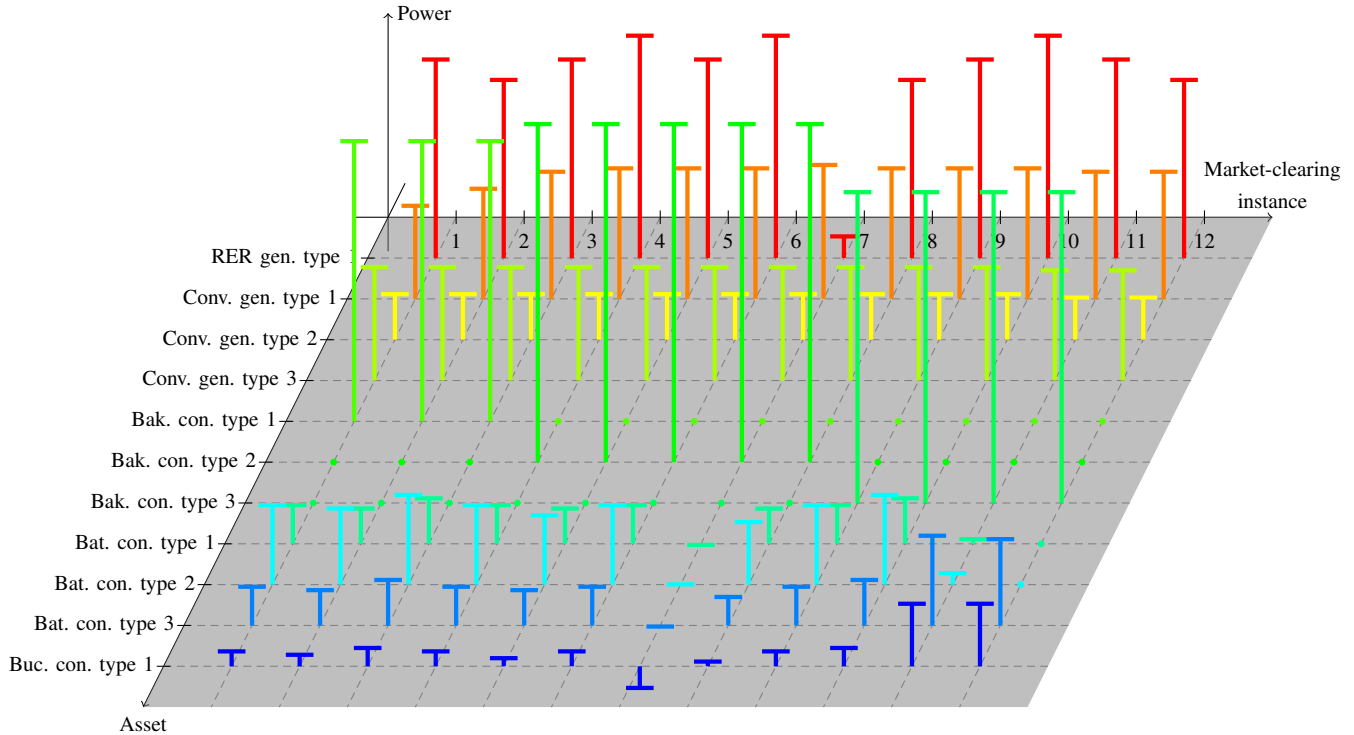


Fig. 11. Accumulated power levels of market-clearing results during one hour with a 5 minute market-clearing time in a system with 15% RER penetration level, BBB flexibility configuration and 90% RER generation availability drop. Dots, such as Bakery consumption type 2 at market-clearing instance 1, indicate a power level of zero while any power level different from zero is indicated by a horizontal bar at the end of a vertical line.

any price driven incentive signal for the generators and consumers to react on. One such example is Critical Peak Pricing (CPP). In a system with CPP, the price is manually raised to encourage lower consumption during critical scenarios. For example, in the scenarios addressed in Cases *S1*, *S2*, and *S3* a critical scenario, the price could be raised for the duration of the weather situation. If done intelligently, the positives of a CPP approach is the overall lowered risk of system instability as consumption reduces and the dependency on intermittent and uncertain generation reduces. However, CPP is an open-loop control approach and as such cannot be guaranteed to reduce consumption by the needed amount. In a system with flexible consumers such as the BBB, a CPP approach must be carefully designed such that the peak price utilizes the flexibility of Bucket and Battery consumers correctly, i.e., the price must be such that Batteries turn off just the right amount and Buckets act as generators at just the right time. In contrast, with the DMM approach and the use of LMP arrived at through iterative negotiations, the prices and the time instants can be determined automatically through closed-loop actions and utilize all flexibilities available.

In [41], a wide variety of pricing strategies are discussed thoroughly and the advantages and disadvantages of each is presented. Real-Time Pricing comes out of this discussion as the pricing strategies with the highest potential, but as pointed out in [17] adoption of Real-Time Pricing comes with a risk of adding instability to a system which has to be dealt with

carefully. The results of this paper, and the stability conditions articulated in Theorem 1, can be viewed as a guideline for pricing strategies that avoid such instabilities.

VI. CONCLUDING REMARKS

In this paper, we have proposed a dynamic market mechanism for wholesale electricity markets with different classes of flexible demand response-compatible units, renewable generators, and an ISO that determines the economic dispatch. Conditions under which this DMM is stable and the region of attraction are delineated and its performance is validated using an IEEE 118 Bus, a high-fidelity simulation of the the Midwestern US Power Grid. The defining feature of the DMM, namely the negotiation process between all market players, is shown to result in increased Social Welfare, when compared to the standard OPF tool, in the presence of uncertainties in RER generators. The DMM not only demonstrates the flexibility of the different classes of consumption units, Buckets, Batteries and Bakeries which help mitigate the negative impacts from intermittent RER generators, but also determines the desired combination of BBB as the levels of intermittency and penetration increase, and the corresponding increases in Social Welfare.

While all results derived are applicable to the wholesale electricity market, which is pool-based and ISO-centric, the fundamental principles of DMM have the potential to be applied to bilateral as well as retail markets which need to be

TABLE VI

SOCIAL WELFARE IMPROVEMENTS IN S1. FLEXIBILITY CONFIGURATION B IS BAKERY ONLY, BB IS BAKERY PLUS BATTERY, AND BBB IS BAKERY, BATTERY PLUS BUCKET. THE SOCIAL WELFARE OF 15% RER PENETRATION LEVEL WITH ONLY BAKERY CONSUMPTION IS USED AS REFERENCE.



TABLE VII

SOCIAL WELFARE IMPROVEMENTS IN S2. FLEXIBILITY CONFIGURATION B IS BAKERY ONLY, BB IS BAKERY PLUS BATTERY, AND BBB IS BAKERY, BATTERY PLUS BUCKET. THE SOCIAL WELFARE OF 15% RER PENETRATION LEVEL WITH ONLY BAKERY CONSUMPTION IN FIG. VI IS USED AS REFERENCE.

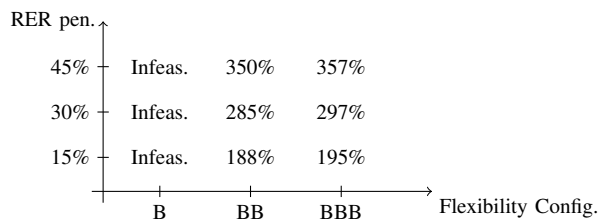
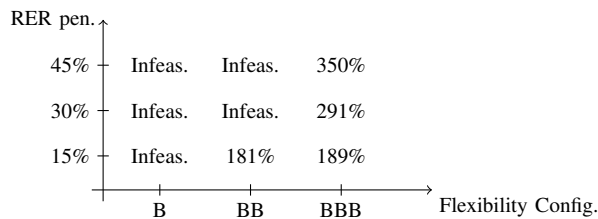


TABLE VIII

SOCIAL WELFARE IMPROVEMENTS IN S3. FLEXIBILITY CONFIGURATION B IS BAKERY ONLY, BB IS BAKERY PLUS BATTERY, AND BBB IS BAKERY, BATTERY PLUS BUCKET. THE SOCIAL WELFARE OF 15% RER PENETRATION LEVEL WITH ONLY BAKERY CONSUMPTION IN FIG. VI IS USED AS REFERENCE.



increasingly engaged as more analytics and decision-making enter the distribution and demand side entities in the electricity grid.

APPENDIX A

CONSUMER AND GENERATOR CONSTANTS

This appendix provides the consumer and generator constants used for the case studies described in Section IV. Table IX, X, and XI provide Bucket, Battery, and Bakery consumer constants, respectively. Table XII provide conventional and RER generator constants.

REFERENCES

[1] J. Hansen, J. Knudsen, A. Kiani, A. M. Annaswamy, and J. Stoustrup, "A Dynamic Market Mechanism for Markets with Shiftable Demand Response," *Proceedings of the 19th IFAC World Congress*, 2014.

TABLE IX
BUCKET CONSUMER CONSTANTS.

Type	\underline{P}_{Dc} [MW]	\overline{P}_{Dc} [MW]	\underline{E}_{Dc} [MW]	\overline{E}_{Dc} [MW]	b_{Dc}	c_{Dc}
1	-75	75	-100	100	119	-0.1

TABLE X
BATTERY CONSUMER CONSTANTS.

Type	\underline{P}_{Dt} [MW]	\overline{P}_{Dt} [MW]	\overline{E}_{Dt} [MW]	T_{end} [min]	b_{Dt}	c_{Dt}
1	0	50	150	60	120	-0.1
2	0	60	300	60	120	-0.05
3	0	55	220	60	120	-0.1

TABLE XI
BAKERY CONSUMER CONSTANTS.

Type	\overline{P}_{Dk} [MW]	\overline{E}_{Dk} [MW]	T_{end} [min]	T_{run} [min]
1	50	150	15	15
2	60	300	40	25
3	55	220	60	20

TABLE XII
CONVENTIONAL (CLASS 1) AND RER (CLASS 2) GENERATOR CONSTANTS.

Class	Type	\underline{P}_G [MW]	\overline{P}_G [MW]	$\underline{R}_G \frac{[MW]}{T_s}$	$\overline{R}_G \frac{[MW]}{T_s}$	b_G	c_G
1	1	0	150	-5	5	15	2.5
1	2	0	100	-20	20	40	5
1	3	0	100	-10	10	25	4
2	1	0	100	-100	100	10	0

- [2] D. Olsen, S. Goli, D. Faulkner, and A. McKane, "Opportunities for Automated Demand Response in Wastewater Treatment Facilities in California - Southeast Water Pollution Control Plant Case Study," LBNL, Tech. Rep. 6056E, 2012.
- [3] J. J. Kim, R. Yin, and S. Kiliccote, "Automated Price and Demand Response Demonstration for Large Customers in New York City using OpenADR," LBNL, Tech. Rep. 6472E, 2013.
- [4] J. Hansen, J. Knudsen, and A. M. Annaswamy, "Demand Response in Smart Grids: Participants, Challenges, and a Taxonomy," *53rd IEEE Conference on Decision and Control*, 2014.
- [5] B. Biegel, P. Andersen, T. S. Pedersen, K. M. Nielsen, J. Stoustrup, and L. H. Hansen, "Smart Grid Dispatch Strategy for ON/OFF Demand-Side Devices," *European Control Conference*, 2013.
- [6] M. K. Petersen, L. H. Hansen, J. Bendtsen, K. Edlund, and J. Stoustrup, "Market Integration of Virtual Power Plants," *52nd IEEE Conference on Decision and Control*, 2013.
- [7] F. C. Schweppe, M. C. Caramanis, R. D. Tabors, and R. E. Bohn, *Spot Pricing of Electricity*. Kluwer Academic Publishers, 1988.
- [8] D. S. Kirschen, G. Strbac, P. Cumperayot, and D. de Paiva Mendes, "Factoring the elasticity of demand in electricity prices," *Power Systems, IEEE Transactions on*, vol. 15, no. 2, pp. 612–617, May 2000.
- [9] A.-H. Mohsenian-Rad and A. Leon-Garcia, "Optimal Residential Load Control With Price Prediction in Real-Time Electricity Pricing Environments," *IEEE Transactions on Smart Grid*, vol. 1, no. 2, 2010.
- [10] Z. Chen, L. Wu, and Y. Fu, "Real-Time Price-Based Demand Response Management for Residential Appliances via Stochastic Optimization and Robust Optimization," *IEEE Transactions on Smart Grid*, vol. 3, no. 4, 2012.

- [11] K. Ma, G. Hu, and C. J. Spanos, "Distributed Energy Consumption Control via Real-Time Pricing Feedback in Smart Grid," *IEEE Transactions on Control Systems Technology*, vol. 22, no. 5, pp. 1907–1914, Sept 2014.
- [12] A. K. Bejestani and A. Annaswamy, "A Dynamic Mechanism for Wholesale Energy Market: Stability and Robustness," *IEEE Transactions on Smart Grid*, vol. 5, no. 6, 2014.
- [13] F. L. Alvarado, J. Meng, C. L. DeMarco, and W. S. Mota, "Stability Analysis of Interconnected Power Systems Coupled with Market Dynamics," *IEEE Transactions on Power Systems*, vol. 16, no. 4, 2001.
- [14] R. Sioshansi and A. Tignor, "Do Centrally Committed Electricity Markets Provide Useful Price Signals?" *The Energy Journal*, vol. 33, no. 4, 2012.
- [15] R. Baldick, "Computing the Electricity Market Equilibrium: Uses of market equilibrium models," *Power Systems Conference and Exposition*, 2006.
- [16] Q. Huang, M. Roozbehani, and M. A. Dahleh, "Efficiency-Risk Tradeoffs in Electricity Markets with Dynamic Demand Response," *IEEE Transactions on Smart Grid*, vol. 6, no. 1, 2015.
- [17] G. Wang, M. Negrete-Pincetic, A. Kowli, E. Shafiepoorfar, S. Meyn, and U. Shanbhag, "Real-time Prices in an Entropic Grid," *Innovative Smart Grid Technologies*, 2012.
- [18] P. Chakraborty and P. P. Khargonekar, "Impact of Irrational Consumers on Rational Consumers in a Smart Grid," *American Control Conference*, 2014.
- [19] S. Bashash and H. K. Fathy, "Modeling and Control of Aggregate Air Conditioning Loads for Robust Renewable Power Management," *IEEE Transactions on Control Systems Technology*, vol. 21, no. 4, 2013.
- [20] Z. Ma, D. S. Callaway, and I. A. Hiskens, "Decentralized Charging of Large Populations of Plug-in Electric Vehicles," *IEEE Transactions on Control Systems Technology*, vol. 5, no. 4, 2014.
- [21] M. Parvania, M. Fotuhi-Firuzabad, and M. Shahidehpour, "Optimal Demand Response Aggregation in Wholesale Electricity Markets," *IEEE Transactions on Smart Grid*, vol. 4, no. 4, 2013.
- [22] D. E. Olivares, A. Mehrizi-Sani, A. H. Etemadi, C. A. Cañizares, R. Iravani, M. Kazerani, A. H. Hajimiragha, O. Gomis-Bellmunt, M. Saadefard, R. Palma-Behnke, G. A. Jiménez-Estévez, and N. D. Hatziargyriou, "Trends in Microgrid Control," *IEEE Transactions on Smart Grid*, vol. 21, no. 1, 2013.
- [23] H. Dagdougui and R. Sacile, "Decentralized Control of the Power Flows in a Network of Smart Microgrids Modeled as a Team of Cooperative Agents," *IEEE Transactions on Control Systems Technology*, vol. 22, no. 2, 2014.
- [24] A. Ouammi, H. Dagdougui, and R. Sacile, "Optimal Control of Power Flows and Energy Local Storages in a Network of Microgrids Modeled as a System of Systems," *IEEE Transactions on Control Systems Technology*, vol. 23, no. 1, pp. 128–138, Jan 2015.
- [25] F. C. Schweppe, R. D. Tabors, and J. L. Kirtley, "Homeostatic Control: The Utility/Customer Marketplace for Electric Power," *MIT Energy Laboratory Report MIT-EL 81-033*, 1981.
- [26] D. S. Kirschen and G. Strbac, *Fundamentals of Power System Economics*. John Wiley & Sons Inc., 2004.
- [27] W. W. Hogan, "Contract Networks for Electric Power Transmission," *Journal of Regulatory Economics*, vol. 4, 1992.
- [28] www.iso-ne.com, "ISO New England Issues Annual Power System Plan for New England."
- [29] Department of Public Utilities, "Investigation by the Department of Public Utilities on its own Motion into Modernization of the Electric Grid," *D.P.U. 12-17-B*, June 12 2014.
- [30] D. Turner, "Day-Ahead Energy Markets: Introduction to Wholesale Electricity Markets (WEM 101)," ISO New England, Northampton, MA, Tech. Rep., September 2014.
- [31] M. H. Albadi and E. F. El-Saadany, "Demand Response in Electricity Markets: An Overview," *IEEE Power Engineering Society General Meeting*, 2007.
- [32] H. W. Dommel and W. F. Tinney, "Optimal Power Flow Solutions," *Power Apparatus and Systems*, *IEEE Transactions on*, vol. PAS-87, no. 10, pp. 1866–1876, Oct 1968.
- [33] www.iso-ne.com, "2014 Regional Electricity Outlook."
- [34] Energy & Environmental Economics, "A Survey of Time-of-Use (TOU) Pricing and Demand Response (DR) Programs," 2005.
- [35] E. Y. Bitar, R. Rajagopal, P. P. Khargonekar, K. Poolla, and P. Varaiya, "Bringing wind energy to market," *IEEE Transactions on Power Systems*, vol. 27, no. 3, 2012.
- [36] G. Giebel, P. Soerensen, and H. Holtinen, "Forecast error of aggregated wind power," Tech. Rep., April 2007.
- [37] M. C. Caramanis and J. M. Foster, "Uniform and complex bids for demand response and wind generation scheduling in multi-period linked transmission and distribution markets," *50th IEEE Conference on Decision and Control*, 2011.
- [38] K. J. Arrow, L. Hurwicz, and H. Uzawa, *Studies in Linear and Non-Linear Programming*. Stanford University Press, Stanford, California, 1958.
- [39] D. P. Bertsekas, *Nonlinear Programming*. Athena Scientific, Belmont, Massachusetts, 1999.
- [40] P. Sorensen, N. A. Cutululis, A. Viguera-Rodríguez, L. E. Jensen, J. Hjerrild, M. H. Donovan, and H. Madsen, "Power Fluctuations From Large Wind Farms," *IEEE Transactions on Power Systems*, vol. 22, no. 3, pp. 958–965, 2007.
- [41] S. Borenstein, M. Jaske, and A. Rosenfeld, "Dynamic Pricing, Advanced Metering, and Demand Response in Electricity Markets," *Center for the Study of Energy Markets*, 2002.



Jesper Knudsen was born in Aalborg, Denmark, in 1989. He received the B.Sc and M.Sc degrees in electronic engineering and IT from Aalborg University in 2012 and 2014, respectively.

From August 2014 to January 2015, he was a Research and Development Engineer with the Danish company DEIF that develops control solutions for decentralized power generators. Since January 2015, he has been an Industrial PhD Fellow with Aalborg University in collaboration with DEIF. His research interests include power systems, control systems,

smart grid, and automation in a wide perspective.

Mr. Knudsen was the recipient of the Bikuben - DAF Fellowship (Denmark-America Foundation) in 2013.



Jacob Hansen was born in Denmark and received his B.Sc and M.Sc degrees in electronic engineering and IT from Aalborg University in 2012 and 2014, respectively.

During his M.Sc studies, he was a Visiting student with the Department of Mechanical Engineering, at Massachusetts Institute of Technology (MIT) in Cambridge MA.

His research interests include smart grid, power systems, decentralized control, and control systems in general.

Mr. Hansen was the recipient of the GN Store Nord - DAF Fellowship (Denmark-America Foundation) in 2013.



Dr. Anuradha Annaswamy received the Ph.D. degree in Electrical Engineering from Yale University in 1985. She has been a member of the faculty at Yale, Boston University, and MIT where currently she is the director of the Active-Adaptive Control Laboratory and a Senior Research Scientist in the Department of Mechanical Engineering. Her research interests pertain to adaptive control theory and applications to aerospace and automotive control, active control of noise in thermo-fluid systems, control of autonomous systems, decision and control in smart grids, smart cities, and critical infrastructures, and co-design of control and platform architectures in cyber physical systems.

Dr. Annaswamy has received several awards including the George Axelby and Control Systems Magazine best paper awards from the IEEE Control Systems Society, the Presidential Young Investigator award from the National Science Foundation, the Hans Fisher Senior Fellowship from the Institute for Advanced Study at the Technische Universität München in 2008, and the Donald Groen Julius Prize for 2008 from the Institute of Mechanical Engineers. Dr. Annaswamy is a Fellow of the IEEE and a member of AIAA.